Summer 9-1-2014

Phosphorylation Regulation of T-Lymphocyte Migration

Xiaolu Xu
Washington University in St. Louis

WASHINGTON UNIVERSITY IN ST. LOUIS

Division of Biology & Biomedical Sciences

Immunology

Dissertation Examination Committee:

Yina Huang, Chair

John Cooper

Gregory Longmore

S. Celeste Morley

Gwendalyn Randolph

Andrey Shaw

Phosphorylation Regulation of T Lymphocyte Migration

by Xiaolu Xu

A dissertation presented to the
Graduate School of Arts and Sciences
of Washington University in
partial fulfillment of the
requirements for the degree
of Doctor of Philosophy

August 2014

St. Louis, Missouri

TABLE OF CONTENTS

Page

Page

ACKNOWLEDGMENTS

I would love to acknowledge my thesis mentor Dr. Yina H. Huang for providing funding, laboratory space, equipment, and instructions for completing the work presented here. I would also love to acknowledge Xinxin Wang, Nancy Mathis, Jiancheng Hu, Teerawit Supakorndej, Yunfeng Feng, Elizabeth Todd, and Emily Jaeger for providing significant technical support. I would also love to acknowledge Dr. Andrey Shaw, Dr. John Cooper, Dr. Gregory Longmore, Dr. Celeste Morley, and Dr. Gwendalyn Randolph for providing guidance and critique for me and my work.

ABSTRACT OF THE DISSERTATION

Phosphorylation Regulation of T Lymphocyte Migration

by

Xiaolu Xu

Doctor of Philosophy in Biology and Biomedical Sciences

Immunology

Washington University in St. Louis, 2014.

Professor Yina H. Huang, Chair

Immune surveillance requires efficient trafficking of leukocytes throughout the body. To achieve this, leukocytes have evolved to be highly migratory and responsive to environmental cues, which provide guidance for proper tissue distribution. The translation of external environmental cues to intracellular physical changes in leukocytes requires a cascade of receptors, signal transducers, and mechanical effectors. My doctoral research focused on using T-cells as a model to study the unique cellular process of how signal transducers interact with and regulate mechanical effectors in fast migrating immune cells. Specifically, it is known that the signal transducer Mst1 kinase is required for T-cell polarization, adhesion, and active migration, but the underlying mechanisms remain poorly understood. I have demonstrated that Mst1 regulates

two mechanical effectors, the molecular motor Myosin-IIA and the cytoskeleton regulatory protein L-plastin, through the process of phosphorylation. The regulation of Myosin-IIA enables it to generate contractile force inside a migrating T-cell, maintaining the shape and proper adhesion of the cell to extracellular matrix, both being requirements for successful migration. The regulation of L-plastin enables it to activate integrin adhesion molecules as well as to properly organize lamellipodial actin. In addition, I have identified novel adhesion structures in T-cells called microadhesions, which potentially provide traction force to migrating T-cells. Overall, my research has identified a novel pathway acting between a signal transducer and two mechanical effectors in T-cell migration.

1. INTRODUCTION

Mammalian immune systems are characterized by an abundance of various types of cells that carry out a wide variety of effector functions. In order to distribute the proper cell types to locations, the immune system has evolved a full spectrum of mechanisms to guide them. These mechanisms include specific chemokines which direct migration direction [1–4], adhesion molecules which control tssue retention [1, 5–8]. Their respective signaling pathways translate extracellular cues to intracellular changes [9–14] that control cell morphology and molecular machinery for motility [15–19].

My doctoral dissertation attempts to answer a very fundamental question: how are these different mechanisms interconnected and functioning as an integrated unit so that thymus-dependent lymphocytes (T-lymphocyte or T-cell) can properly home to their proper locations.

1.1 Cellular Adhesion and Motility

Cellular adhesion and motility are most well studied in slow moving mesenchymal cells such as fibroblasts [20]. The cytoskeleton of these cells exhibit multiple features, including ventral stress fibers, focal adhesions, dorsal fibers, actin arcs [13, 21–25]. Focal adhesion is the main adhesive structure for slow-

migrating cells [25,26]. They are protein complexes varying in size and protein content. But in general, they all share some of the same core proteins, such as F-actin, integrin, vinculin, α-actinin, talin, and paxillin. Focal adhesions are highly organized structures [27–29]. Kanchanawong and colleagues used double tagged quantitative super-resolution fluorescent microscopy to determine the layer of proteins in the structure [30] (Figure 1.1). The first layer, most distal to plasma membrane, is actin stress fiber layer, consisting of F-actin filaments bundled by α-actinin into thick fibers. The second layer is actin regulatory layer, consisting of F-actin bundles, VASP and zyxin. The third layer is the force transduction layer, consisting of talin and vinculin. The fourth layer is the integrin signaling layer, consisting of cytoplasmic tails of integrin α and β chains as well as focal adhesion kinase (FAK). Between fourth and fifth layer is plasma membrane. The fifth layer is the ectodomain of integrin α and β chains and the extracellular matrix bound to integrin.

Focal adhesion formation is a multiple step process. It starts with rapidly turning-over nascent adhesions. Nascent adhesions form behind the edge of spreading lamellipodia. They turn over rapidly, usually lasting for only 10 minutes before disassembly. However, a small fraction of nascent adhesions do not disassemble, but instead extend centripetally and mature into mature focal adhesions. Even though nascent adhesion formation does not depend on myosin activity, maturation of it does. Interestingly, it is not the contractility but actin-bundling activity of myosin that is required for maturation of

nascent adhesions, which can be substituted by α-actinin [22]. Substratum density and tension also seem to affect the size and number of focal adhesions [22]. The presence of mature and stable stress fiber, focal adhesion, and their associated adpator, and mechanical and signaling transducers, may be what governs the behavior of slow migrating cells, and distinguishes them from rapidly-migrating immune cells.

From a mechanical point of view, cell motility is dependent on both adhesive and traction forces and the arrangement of them. In a model of migration, a migrating cell needs to distribute high adhesion to the front end and low adhesion to the back end, while exerting contraction in between such that the front end is fixated on the substratum while the back end can be pulled forward. At the same time, polymerization of G-actin at the front end drives the plasma membrane forward and establishes adhesion at the front. Myosin-dependent contraction detaches adhesions at the back. This constitutes a cyclical process of attachment, detachment, contraction and advancement [20, 31]. In rapid moving T-cells, this model has received support from the evidence that low-affinity integrin is predominantly localized and clustered at the trailing edge [32], whereas extended form of intermediate-affinity integrin is localized to the leading edge of the cell [33]. What is interesting is that a large proportion of T-cell mid-body is enriched with high-affinity integrin, regardless of ligand density [33, 34]. This suggest that instead of requiring a high affinity adhesion at the lamellipodial leading edge. The major site of ad-

hesion is at the center of the cell. This notion is supported by the ruffling that occurs at the lamelipodia, a direct result of lower or less productive adhesion at lamellipodia compared to the mid-body [35], and a less than 1:1 ratio of migration distance to actin-polymerization [25].

The cyclical migration model also stipulates that cell polarity needs to be established before a cell can migrate. Polarity is established by the redistribution of uniformly distributed proteins to locally concentrated sites. For example, regulators of F-actin polymerization and bundling, adhesion such as Arp2/3, α-actinin, high-affinity integrin are concentrated at the front end (hereafter referred to as leading edge) of a cell, while regulators of contraction and low affinity integrin need to concentrate at the back end (hereafter referred to as trailing edge) [32]. Receptors and regulators are actively redistributed and the local clustering of proteins leads to a sufficient concentration to promote downstream functions, such as nucleation of actin by mDia for rapid polymerization, clustering of intermediate- and high-affinity integrin for firm adhesion, concentration of myosin motor protein for effective contraction. Whether the initiation of polarization is a random process is debatable, but this process turns a random system into an organized one [12, 16, 36–39].

Once molecular polarity has been established, the next step in polarization and cell spreading requires mechanical work to contort the spherical cell body into an elongated shape as well as push the cell body so that it can spread out on substratum. This process requires both F-actin polymerization and

myosin contractility. F-actin arcs are centripetally distributed between the lamellipodia and cell body [21]. These arcs are constricted by myosin to form rings around the spherical cell body and exert a force to reshape the cell body into a spread shape. Without F-actin, as in cells treated with cytochalasin, or without myosin-exerted contractility, as in cells lacking myosin II or treated with blebbistatin (myosin ATPase inhibitor) [16, 40], cells instantly re-assume a spherical shape, where the force is evenly distributed throughout the entire cell body resulting in the lowest entropy [23]. This indicates that both F-actin and myosin are required for cell polarity and spreading.

1.2 Integrin Activation, Clustering and Signaling

There are two modes of integrin signaling: inside-out and outside-in. Despite its name, inside-out signaling actually starts from outside of the cell, such as chemokine-chemokine receptor interaction. The chemokine receptor transduces signals through a cascade of molecules, including PLCγ, CalDAG-GEFI, Rap1 GTPase, RAPL, Mst1, RIAM, ADAP, Skap-55, kindlin among others, resulting in the talin-dependent spatial separation of integrin αL and β2. This change translates into unfolding of the integrin ectodomains to allow for high-affinity integrin-ligand binding. In addition to biochemical cues, physical tensioncan also induces activation of integrin affinity maturation and resultant firm adhesion. Rearward flow of actin induced by myosin contraction at lamellipodium associates with recruitment of structural proteins such

as VASP to newly established nascent adhesions [18,26,32]. Shear flow in blood vessels has also been shown to induce conformational activation of leukocyte integrin LFA-1 because it is thermodynamically most stable [8, 41, 42].

One of the most well studied signaling cascade that leads to integrin activation is Rap1-RAPL axis (Figure 1.2). Rap1 is a small GTPase that is downstream of various signals, including T-cell receptor engagement [43], CD31 stimulation [44], CD98 ligation [45], and chemokine receptor engagement [46]. It is activated by various guanine exchange factors, including C3G, PDZ-GEF, CD-GEFI, CD-GEFIII, Repac, and, most importantly, Epac, that is directly activated by cAMP [47]. Rap1 is stored in small intracellular vesicles during resting state, but quickly localize to plasma membrane via a membrane anchor in a Skap-55 dependent manner [48]. Rap-GTP recruits effector protein RAPL via Rap1-binding domain on RAPL, associates with LFA-1 and may mediate Rap1-dependent LFA-1 redistribution via a double lysine (K1097/K1099) motif in the α_L chain of LFA-1 integrin [49–52].

Whereas inside-out signaling is required for integrin activation and cell adhesion, outside-in signaling leads to cell spreading, actin rearrangement, focal adhesion formation and tyrosine phosphorylation [53]. Outside-in signaling starts with integrin-ligand binding, separation of α and β chains, activation of Src family kinases, which activate focal adhesion kinase (FAK) or its hematopoietic analog, Pyk2, culminating in macromolecular complex forma-

tion, focal adhesion generation, actin rearrangement, stress fiber formation, and cell spreading [8, 28, 54–57].

Integrin clustering also increases adhesion by increasing local integrin density, an efficient way of regulating binding valency. Clustering is essential in T and B cell immune synapse formation so that antigen receptors can bind a relatively small amount of ligands on antigen-presenting cells efficiently [58]. Clustering can be induced by both inside-out and outside-in signaling [59], as well as multivalent antibody binding [60]. Transmembrane domains of integrin α and β chains can promote clustering by homotypic oligomerization [60].

1.3 Immune Cell Extravasation and Interstitial Migration

Immune cells are unique in that they can migrate at a speed up to 100 fold faster than sessile mesenchymal cells. Unlike mesenchymal cells which are subject to *anoikis*, or anchorage-dependent survival mechanism [61], lymphocytes are largely autonomous in their environment and do not require constant anchorage for survival. This property makes leukocyte locomotion more similar to the lower eukaryote *Dictyostelium discoideum*, instead of mesenchymal cells [36]. These distinct properties contribute to immune cell's ability to distribute quickly and independently of surrounding tissues to different sites of the body where they are required [20].

Extravasation is the process whereby leukocytes exit from circulation across vascular endothelial barrier into secondary lymphoid organs or inflamed tis-

sue. Post-capillary venules within lymph nodes or Peyer's Patch develop into high endothelial venules (HEV) that are characterized by cuboidal vascular endothelial cells that enable leukocyte attachment and transmigration. HEV expresses important adhesive molecules including peripheral node addressin glycoproteins such as CD34, integrin ligands such as intercellular adhesion molecule-1 (ICAM-1) or ICAM-2, mucosal specific L-selectin ligand MAdCAM-1, and chemokines such as soluble CCL19 and CCL21 bound to endothelial cells via heparan sulfate [7, 62, 63].

Extravasation into inflammatory sites is induced following activation of endothelial cells by IL-1 TNF-α and other inflammatory cytokines secreted by macrophages. Once activated, endothelial cells express addressin, GlyCAM-1, ICAM-1 and other adhesion molecule ligands, and hold chemokine such as CCL2 [64] which are stored inside vesicle in activated endothelial cells. Circulating leukocytes roll on and attach to endothelial cells via L-selectin-Lewis sialyl X interaction [65], and chemokine stimulation triggers integrin inside-out signaling that ends with integrin activation and firm attachment to endothelial layer under shear flow stress. Combined effect of chemokine and shear flow is required for efficient initiation of trans-endothelial migration.

Once inside the tissue, 3-dimensional interstitial migration occurs. CCR7 directs T cells to paracortical T cell zone, and CXCR5 directs B cells to B cell follicles. Using full integrin-ablated mice, it has been shown that integrin-dependent adhesion is not required for lymphoid organ localization, neither

is it required for interstitial migration for dendritic cells. Consistent with this, integrin-blockade with soluble antibodies only slightly decreased B cell interstitial migration within lymph node. In contrast, contractility has been shown to be crucial for efficient interstitial migration in that defect in myosin function results in significantly decreased migration within lymph nodes and dense but not loose matrigel [50, 66, 67].

1.4 Hippo Pathway and Its Role in Mechanosensing

Hippo pathway has been shown to be important in various physiological processes (Figure 1.3), including apoptosis, cell growth and proliferation, organ size control [68], and mechanosensing [69, 70]. Even though these are seemingly distinct processes, they, in fact, constitute a central pathway that senses chemical and mechanical signals, and translates them into intracellular changes of cell death, growth and migration.

Hippo pathway components include Hippo kinases (Mst1/Mst2 kinases) complexed with Salvador (Sav1), Lats1/2 kinase-Mob1 complex, Yorkie-homologues YAP (Yes-associated protein) or mammalian paralog TAZ (transcriptional coactivator with PDZ-binding motif) transcription activators. Upon upstream signaling, Hippo kinases phosphorylate and activate LATS kinase, which in term phosphorylates a serine residue on YAP/TAZ. Phosphorylated-YAP/TAZ interact strongly with 14-3-3 protein leading to their cytoplasmic localization [71–73] and subsequent ubiquitination by $SCF^{\beta-TRCP}$ and degradation [74].

There are extensive studies aimed at revealing the upstream signaling cascades that lead to Hippo pathway signaling. G-protein coupled receptors (GPCR), including lysophosphatic acid(LPA)-sphingosine 1-phosphate receptor (S1P1) ligand-receptor pair, have been shown to directly activate LATS and leads to YAP/TAZ nuclear transportation [75]. Chemotactic factors such as CCL19 and CCL21 have also been shown to lead to MST1 phosphorylation [52, 76]. Leukemia inhibitory factor receptor (LIFR) signaling, E-cadherin homotypic binding and cell detachment have also been shown to activated Hippo pathway and suppress breast cancer growth [77–79]. In addition, extracellular matrix rigidity, cell shape, size and the resulting change of tension and F-actin rearrangement also lead to Hippo pathway-YAP/TAZ signaling and gene transcription [69, 70, 73].

In lymphocytes, a number of groups including ours have shown that Mst1 and Mst2 kinases are required for proper thymocyte emigration and efficient interstitial migration [76, 80, 81]. Katagiri *et al* also presented evidence that Mst1 is required for T-cell polarization, integrin clustering, and adhesion under shear flow [52]. From a mechanistic perspective, Mou*et al* proposed that Mst1 phosphorylates Mob1A/B (MOB kinase activator 1), which subsequently activates Dock8, a Rac guanine exchange factor(GEF), that leads to cytoskeleton rearrangement. These studies identify one molecular pathway underlying the migratory defects of Mst1/2-deficient lymphocytes. However, neither of these characterized Mst1 functions primary T-cells. The study by Katagiri *et al* also

mistakenly equates T-cell cytoskeletal polarization with integrin clustering, a proecess requiring T-cell polarization among many others. A T-cell unable to polarize will inevitably be unable to cluster its integrin, therefore it is difficult to gauge whether integrin-clustering *per se* is defective in a system where its prior step has already been disrupted. The study by Mou *et al* was also problematic in that their mechanistic studies were completely carried out in a system (U2OS human osteosarcoma cell line) very dissimilar to T-cells. As mentioned above, rapidly-migrating T-cells behave very differently in migration pattern as compared to slowly-migrating mesenchymal cells. Therefore, it is questionable whether the molecular mechanism determined in U2OS can be applied to T-cells.

1.5 Outstanding Questions

Given the complexity of cell migration and mechanosensing, many questions remain un-addressed at the beginning of this dissertation study. For example, what distinguishes slowly-migrating cells, which form stress fiber and focal adhesion, such as fibroblast, from fast-migrating cells, which do not form stress fiber or focal adhesions, such as lymphocytes, in their respective migratory behavior. Another question is whether Hippo kinase (Mst1 in mammalian cells) functions in the same or different manner in slowly-migrating cells and fast-migrating cells. It has been well demonstrated that Mst1 is required for efficient emigration and migration of T-cells through its regulation of polarity,

and perhaps, integrin and adhesion. However, the Mst1 intermediates and effectors required to achieve its regulatory goals is(are) still obscure. The goal of this thesis is to uncover the mechanisms and effectors of Mst1-dependent polarity/adhesion regulation.

1.6 FIGURES

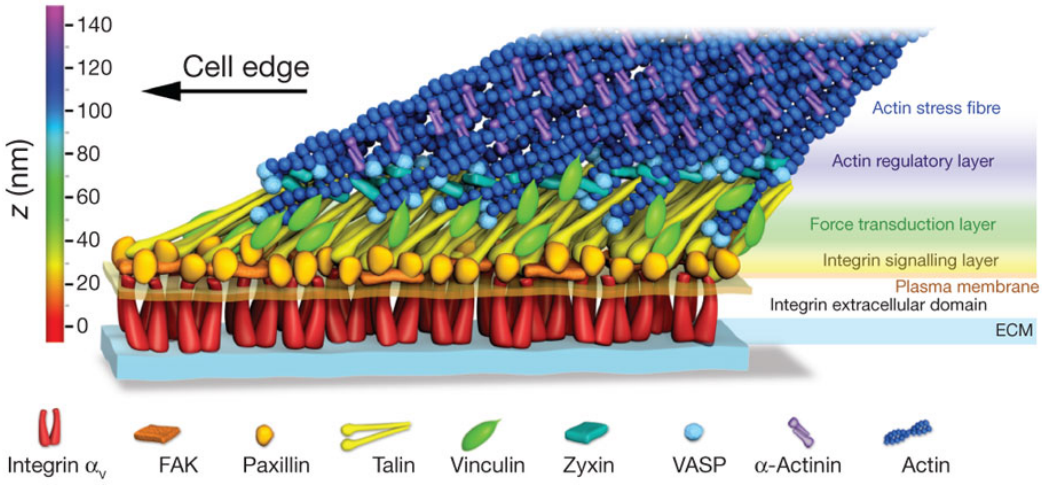

Figure 1.1. Kanchanawong(2010)

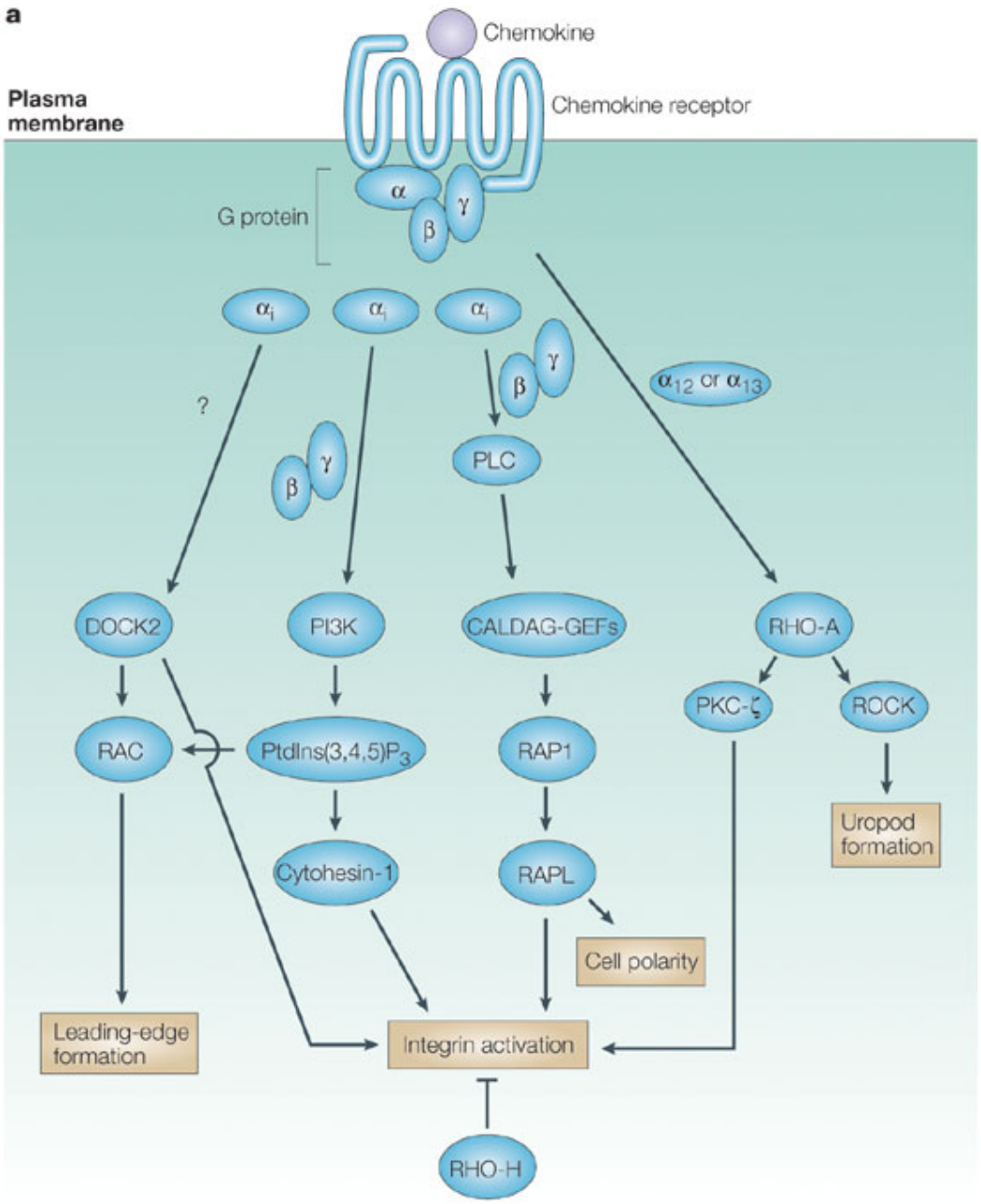

Figure 1.2. Kinashi(2005)

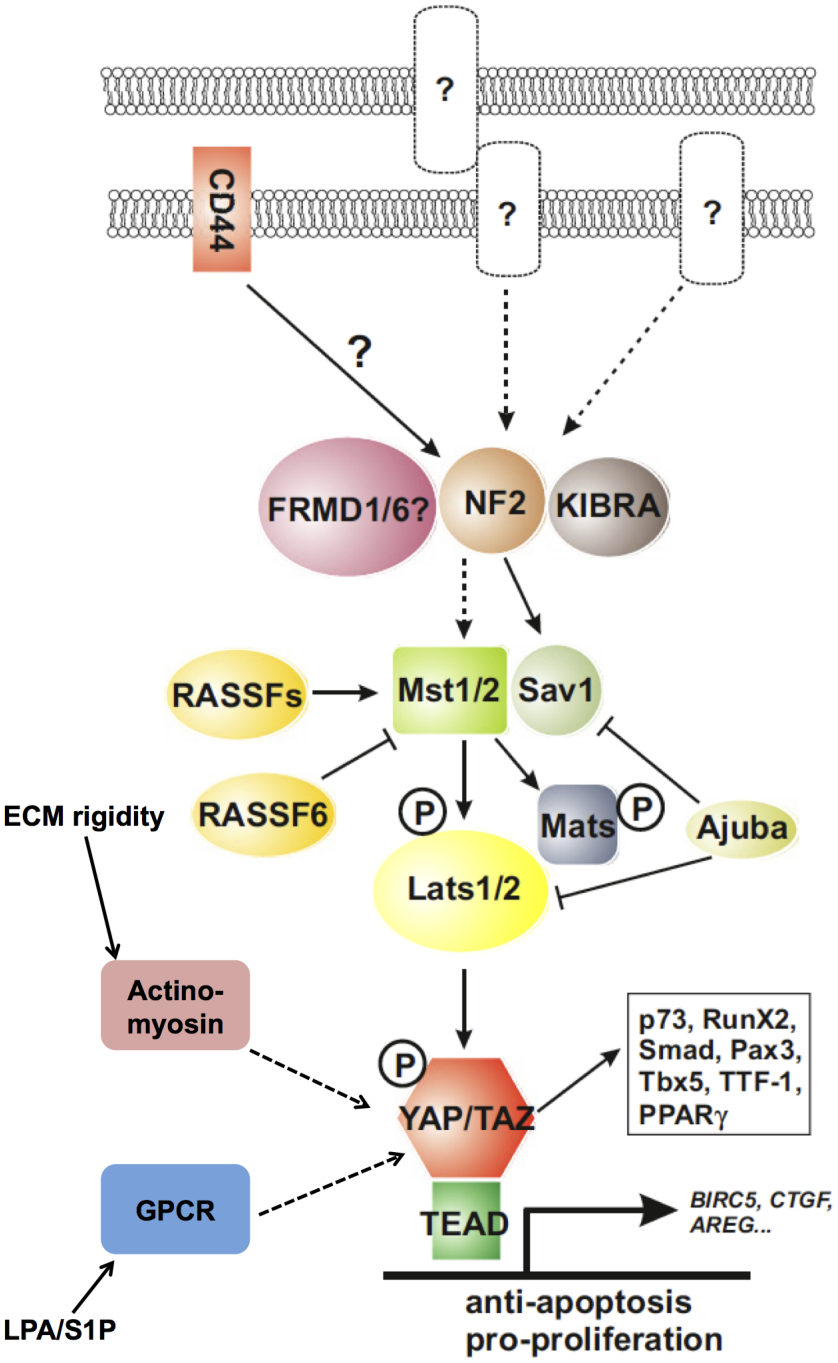

Figure 1.3. Adapted from Pan(2010)

2. Mst1 Directs Myosin IIa Partitioning of Low and Higher Affinity Integrins During T cell Migration

Chemokines promote T cell migration by transmitting signals that induce T cell polarization and integrin activation and adhesion. Mst1 kinase is a key signal mediator required for both of these processes; however, its molecular mechanism remains unclear. Here, we present a mouse model in which Mst1 function is disrupted by a hypomorphic mutation. Microscopic analysis of Mst1-deficient CD4 T cells revealed a necessary role for Mst1 in controlling the localization and activity of Myosin IIa, a molecular motor that moves along actin filaments. Using affinity specific LFA-1 antibodies, we identified a requirement for Myosin IIa-dependent contraction in the precise spatial distribution of low and higher affinity LFA-1 on the membrane of migrating T cells. Mst1 deficiency or myosin inhibition resulted in multipolar cells, difficulties in uropod detachment and diffuse localization of low affinity LFA-1. Mechanistically, we have demonstrated that Mst1 interacts with and phosphorylates Myosin Regulatory Light Chain (MRLC2) at Thr10/11. Thus, Mst1 regulates Myosin IIa dynamics to organize high and low affinity LFA-1 to the anterior and posterior contact-zone during T cell migration.

2.1 INTRODUCTION

Human mutations in the Mst1 gene result in a primary immunodeficiency disease [82–84]. Affected patients experience recurrent viral and bacterial respiratory infections as well as cutaneous lesions resulting from Human Papillomavirus infections. Defective immune protection against these infections is due to T cell deficiency [82–84]. *In vivo* and *in vitro* analyses of Mst1 deficient mice have been instrumental in identifying Mst1 as a key regulator of T cell trafficking [52, 76, 80, 81]. The ability of T cells to continually circulate through the body is critical for immune protection (reviewed in [85]). Different T cell subsets have distinct trafficking patterns. Naive and central memory T cells traffic between the blood and lymphatics. They patrol secondary lymphoid organs such as the spleen and lymph nodes for cognate antigen brought there by tissue-derived antigen presenting cells. In contrast, effector T cells traffic to and within inflamed tissue to promote inflammation and mediate direct target cell killing. T cell trafficking patterns are programmed by the expression of membrane chemokine receptors and adhesion molecules, including selectins and integrins [1]. T cells enter secondary lymphoid organs and peripheral tissue from the vasculature by extravasation. Selectins mediate T cell rolling along the endothelium while integrins provide the strong adhesion required for stopping and squeezing through the endothelium. Within the lymph node, naive and central memory T cells are guided by the chemokines

CCL19 and CCL21 to migrate along fibroblastic reticular cells in an integrin-independent manner. In the absence of antigen, T cells leave the lymph nodes via the lymphatics to downstream lymph nodes and eventually return to the blood. Similarly, effector T cells are recruited to sites of infection by chemotactic cues and extravasate in an integrin-dependent manner. However, unlike within lymphoid organs, inflammation restructures the peripheral tissue environment and up-regulate integrin ligands [86]. Migration of effector T cells within the inflamed tissue is highly dependent on integrins and is completely disrupted by integrin blocking antibodies [86].

T-cell responses to chemokines and integrin activation are critical for migration. Chemokines induce T cell polarization and impart migratory directionality. Integrins mediate adhesion and extravasation through endothelia. Mst1 differentially regulates these processes. Mst1 deficient T cells show defects in CCL19-induced polarization *in vitro* and decreased migratory velocity within lymph nodes and thymus [76, 87]. Mst1 deficiency also leads to significant defects in T cell egress from the thymus and in lymph node entry, demonstrating that Mst1 function is required for extravasation [52, 76, 80, 81, 87]. *In vitro* analysis of adhesion show that while selectin-dependent rolling is unaffected, integrin-dependent firm adhesion is Mst1-dependent [76]. Integrin-mediated adhesion is a highly regulated process. Integrin affinity and avidity are increased by inside-out signaling downstream of the T cell receptor (TCR) or chemokine receptor (CCR) [10]. Inside-out signaling changes the orientations

of the cytoplasmic tails of integrin α and β chains to allow the extracellular domains to adopt higher affinity conformations [9]. In addition, binding avidity increases through clustering of multiple LFA-1 receptors. Activation of the small GTPase Rap1 mediates both increased integrin affinity and avidity [9]. Recently, separate Rap1 effector complexes were identified to associate with the cytoplasmic domains of LFA-1 subunits. RAPL binds directly to the α_L subunit (CD11a) while RIAM in association with Kindlin-3 binds to the β_2 subunit (CD18). Both RAPL and RIAM complexes contain Mst1 and are dependent on ADAP/SKAP55 adapter proteins [88], suggesting that Mst1 may contribute to affinity and avidity maturation. However, ICAM-1-Fc fusion proteins equally stain wt and Mst1 deficient T cells, indicating that LFA-1 affinity activation is Mst1-independent. In contrast, Mst1-deficient T cells show defects in global LFA-1 clustering [52]. This indicates that Mst1 participates in inside-out signaling to regulate integrin clustering, although the underlying molecular mechanism remains elusive.

Integrin affinity differs among topological locations on the membrane of migrating T cells. LFA-1 molecules at the leading edge and mid-body are in the intermediate and high affinity conformations, respectively, while uropodal and trailing edge LFA-1 molecules have low ligand affinity [33, 34, 89]. This allows the leading edge to form nascent adhesive contacts, the mid-body to firmly adhere to establish traction and the trailing edge to detach from the substratum. Although Mst1 does not regulate LFA-1 affinity maturation [52],

it remains to be determined whether Mst1 controls the distribution of different affinity LFA-1 molecules. The actinomyosin contractile module is a well-studied mechanotransduction machine that regulates integrin-dependent and independent migration [90]. The ATP-dependent motor protein, Myosin IIA generates force on filamentous (F-) actin to induce T cell contraction. Myosin-mediated contraction is necessary for the establishment of new adhesion at the lamellipodium and the detachment of low affinity integrins at the uropod [26, 91]. Myosin is also important for integrin-independent migration in interstitial tissue via a cyclical squeezing and pushing mode of movement [40, 66]. More broadly, myosin is required for the maintenance of cell polarity and morphology. Myosin-IIa deficient or inhibited cells are either unable to polarize or become multipolar [92, 93] and are severely defective in migration through intact endothelium and small pores requiring cellular contractility [67, 94]. Here, we demonstrate that Mst1-deficient T cells phenotypically resemble Myosin-IIa-inhibited cells. We report a new role for Myosin IIa in controlling adhesion through the proper spatial distribution of low and high affinity LFA-1 during T cell migration. Additionally, we show that Mst1 acts through Myosin IIa to regulate polarization and adhesion during migration.

2.2 MATERIALS AND METHODS

2.2.1 Mice

Mst1$^{h/h}$ (WeeT) mice were identified by flow cytometric screening of peripheral blood of G3 progeny from C57BL/6 male mice treated with N-ethyl-N-nitrosourea (ENU) as previously described [95, 96]. For phenotypic analysis and mechanistic studies, Mst1$^{h/h}$ mice were backcrossed to wt C57BL/6 mice for 10 generations to remove other ENU-induced mutations. To identify the causative mutation in WeeT mice, affected C57BL/6 mice were bred to 129Sv/ImJ mice to generate hybrid F2 mice for mapping. Single nucleotide polymorphism (SNP) assays across the entire genome (n = 356) were performed using the Sequenom MassARRAY system [97]. Map Manager QTX was used to calculate logarithm of the odds (LOD) scores and perform interval mapping [98]. Sequencing was performed on an Illumina genome analyzer after enriching genomic DNA for the mapped region using a custom Nimblegen array (Short Read Archive # SRA059354). Mice were housed in a specific pathogen-free facility. Experimental protocols were approved by the GNF Animal Study Committee, the Washington University Animal Study Committee (protocol # 20110133) and the Dartmouth College Institutional Animal Care and Use Committee (protocol # huan.yh.1).

2.2.2 Detection of Mst1 transcripts and protein

For Mst1 mRNA detection, cDNA was synthesized from T cells with SuperScript II Reverse Transcription kit (Invitrogen). Quantitative PCR was carried out using SYBR Green Master Mix (Agilent) on a PRISM 7000 Sequence Detection System (Applied Biosystems) using GAPDH and Mst1 primers: 5'-GCAGGCAGCTGAAAAAGTT-3' and 5'-CCATAAGACCCCTCTCCAAG-3'. For Mst1 protein detection, purified CD4+ T cells (Invitrogen) treated with vehicle, MG132 or Z-DEVD were lysed with Triton X-100 lysis buffer ((1% Triton X-100, 50mM Tris pH8.0, 100mM NaCl, proteases inhibitors (Roche). Pre-cleared cell lysates were analyzed by western blot analysis with Mst1 (Cell Signaling) and β-actin (Sigma) antibodies.

2.2.3 Cell staining

For flow cytometric analysis, cells were stained with antibodies against CD8-PE/Cy7, CD45.2-APC750, CD45.1-PerCP/Cy5.5 (eBioscience), Vα11-FITC, CD24-PE, CD62L-Pacific Blue, CD69-PE, CCR7-APC, CD4-APC, (Biolegend). For LFA-1 localization, purified CD4+ T cells were stained with anti-CD44-Alexa488 and anti-CD11a-Alexa647 (M17/4)) and fixed with 4% paraformaldehyde. For live imaging, staining with anti-CD11a-Alexa647 (M17/4)), and anti-CD11a-Alexa546 (2D7) was performed during imaging, at a concentration of 0.08 ng/mL to prevent integrin blockade.

2.2.4 Confocal and TIRF Microscopy and image analysis

Images were captured under a FluoView-1000 laser-scanning confocal microscope (Olympus). For live imaging, cells were kept in Leibovitz's L-15 buffer (Gibco) supplemented with 2% FCS. Captured images and videos were preprocessed in ImageJ (NIH) and analyzed using MATLAB (MathWorks) to detect individual cells and quantify clustering of fluorescently tagged proteins. Single cell detection was performed with custom-built software written in MATLAB. Clustering of protein was quantified on singularly detected cells as described previously [38]. Briefly, mean pairwise distance of the pixels of the top 10% intensity was calculated as D_α. S_l was the mean pairwise distance of the same number of pixels packed together as a 10 by 10 pixel square, as the upper limit of the clustering. S_u was the mean pairwise distance of the same number of pixels uniformly scattered on the cell perimeter, as the lower limit of the clustering. A clustering index was calculated using the following equation:

$C_{idx} = \frac{S_u - D_\alpha}{S_u - S_l}$.

2.2.5 Transwell assay

Purified CD4 T cells were seeded into top chambers over 3 μm or 5 μm transwell filters with 100 ng/mL CCL19 (PeproTech) in the bottom chamber. After 1.5 hrs at 37C, cells were recovered from the lower chamber and counted

by high throughput enabled flow cytometer LSR II (BD). Percentage of migrated cells was determined as a percentage of total input. In some cases, the transwell filters were pre-coated with BSA or 2 μg/mL ICAM-1-Fc (R&D Systems).

2.2.6 *In vitro* kinase assay

Purified recombinant GST-Mst1 kinase domain and GST-MRLC2 or GST-MRLC2 T10/11A were mixed together in the presence of kinase buffer (25 mM Hepes, 10 mM $MgCl_2$, 0.5 mM $NaVO_4$, 0.5 mM DTT) with or without [γ-32P]-ATP. Reactions were terminated after 45 minutes with PAGE sample buffer and boiled for 1 minute before separation by SDS-PAGE. In cases where [γ-32P]-ATP was added, the PAGE gel was stained with Coomassie Blue and visualized by autoradiography.

2.2.7 Luciferase complementation assay

Luciferase complementation assay was carried out as previously described. Briefly, 293T cells were co-transfected with different combinations of Mst1-N-Luc and target-C-Luc fusion constructs with FuGENE 6 (Promega, Madison, WI). One day post transfection, cells were seeded into luciferase plates. Luciferin substrate was added after 12 hours and imaged using an IVIS-200 in vivo imaging system (Caliper Life Sciences, Hopkinton MA).

2.2.8 Statistics

GraphPad Prism was used to perform Student's t-test on normally distributed data and Mann-Whitney or Wilcoxon ranked sum test for non-normally distributed data.

2.3 RESULTS

2.3.1 WeeT mice are T cell deficient due to a mutation in Mst1

In an ENU-mutagenesis screen for genetic mutations resulting in T cell lymphopenia, we identified one pedigree, named WeeT ($Mst1^{h/h}$, see below) with reduced proportions of conventional CD4 and CD8 T cells in the peripheral blood (Figure 2.1(a)). Approximately 25% of G3 progeny were lymphopenic, indicative of a single recessive mutation. CD11b+ myeloid and B220+ B cell proportions were mildly increased. WeeT mice were out-crossed to 129Sv/ImJ mice and F2 progeny were used to map the causative mutation by correlating phenotype and inheritance of C57BL/6 (B), 129Sv/ImJ (C) or both (H, heterozygous) single nucleotide polymorphisms (SNPs) using a SNP panel [96,99]. A perfect genotype-phenotype correlation identified a 4.5 Mb region on chromosome 2 (Figure 2.1(b)). Deep sequencing of genomic DNA following enrichment for exons in the 4.5 Mb region revealed an A to C transversion in exon 5 of the Mst1 gene (Figure 2.1(c)), resulting in substitution of Leu at amino acid position 157 with Arg (L157R). This mutation did not disrupt Mst1 transcript levels (Figure 2.1(d)). Instead, we observed a loss of Mst1 protein, in either its full-length or caspase-cleaved form that did not recover following short-term treatment (4 hours) with proteosome (MG132) or caspase-3 (Z-DEVD) inhibitors (Figure 2.1(e)). Thus, we conclude that the WeeT mutation caused

Mst1 protein loss similar to conventionally-targeted Mst1 deficient mice, and hereafter, we refer to homologous mutant WeeT mice as $Mst1^{h/h}$.

2.3.2 Mst1 mutation abrogates Mst1 function in vivo

To determine whether $Mst1^{h/h}$ resulted in a similar immune phenotype as Mst1 knockout mice, we phenotypically characterized $Mst1^{h/h}$ mice. Similar to conventional Mst1 knockout mice, we observed a 3- and 5-fold reduction in splenic CD4 and CD8 T cells in $Mst1^{h/h}$ versus wt littermate mice (Figure 2.2(a), 2.2(b)). As previously reported for Mst1-deficient mice [52, 81], an accumulation of CD4 and CD8 single positive (SP) thymocytes was observed, particularly affecting $HSA^{low}CD69^{neg}$ emigration-ready SP cells (Figure 2.2(a), 2.2(b)). An even greater decrease in peripheral and concomitant increase in thymic CD4 T cells was observed in Mst1-deficient mice bearing the TCR transgene, 5C.C7 (Figure 2.2(c), 2.2(d)). Thus, the L157R mutation in the Mst1 led to a phenotype similar to complete Mst1 knockout.

2.3.3 LFA-1 engagement compensates for Mst1 deficiency in CCL19-induced T cell polarization

T cells respond to chemotactic cues by spatially redistributing cell surface receptors and signaling molecules to facilitate migration. Polarization of chemokine receptors to the leading edge and accumulation of receptors in-

cluding CD44 in the uropod allow more efficient directional movement [100]. Mst1-deficient T cells are defective in polarization [52, 76]. To better understand how Mst1-loss disrupts polarization, we quantified polarization by calculating CD44 receptor clustering in more than 800 individual T cells based on a modified method [38]. Consistent with previous studies, the degree of CD44 clustering decreased significantly in $Mst1^{h/h}$ T cells stimulated with the chemokine CCL19 (Figure 2.3(a), 2.3(b)). Surprisingly, we did not observe a gross difference between wt and Mst1-deficient cells in clustering of global LFA-1 receptors (Figure 2.3(a), 2.3(b)). These quantitative data confirmed that chemokine-induced T cell polarization is Mst1 dependent.

Chemokine-induced T cell polarization can be enhanced by outside-in integrin signaling, which uses distinct signaling pathways to regulate the actin cytoskeleton [10, 101]. To determine whether Mst1 also plays a role in the outside-in integrin signaling, wt and $Mst1^{h/h}$ CD4 T cells were seeded onto ICAM-1 coated chamber slides prior to CCL19 addition. Polarization was monitored by time-lapse imaging in the presence of low concentrations of fluorescently labeled antibodies against LFA-1 and CD44. Low-dose antibody addition neither inhibited adhesion to ICAM-1 nor led to differences in the migratory behavior compared to unstained wt or $Mst1^{h/h}$ CD4 T cells. Interestingly, ICAM-1 engagement of LFA-1 leads to normal CCL19-induced polarization of $Mst1^{h/h}$ CD4 T cells, and enhancement of LFA-1 clustering in both wt and $Mst1^{h/h}$ CD4 T cells (Figure 2.4(a), 2.4(b)). This indicates that

Mst1 is required for T cell polarization in response to chemokine signaling but dispensable for polarization induced by outside-in integrin signaling.

2.3.4 Mst1 is important for cellular contractility

To directly investigate the requirements for Mst1 in chemokine-induced migration, we first assessed the ability of CCL19 to induce CD4 T cell migration through transwell membranes. Broad defects in migration can be detected by evaluating migration through 5 μm pores. Specific defects in cellular contractility can be detected by further evaluating migration through 3 μm pores [67]. CCL19 induced a 8-fold increase in the migration of wt CD4 T cells through either 3 or 5 μm transwell pores compared to chemokine-free controls (Figure 2.4(c)). In contrast, CCL19 induced only a 1.6-fold increase in the migration of Mst1$^{h/h}$ CD4 T cells through 5 μm pores and no detectable migration through 3 μm pores despite normal expression of CCR7 (Figure 2.4(c), 2.4(d)). This general migration defect is consistent with the inability of Mst1$^{h/h}$ T cells to establish cell polarity in response to chemokine stimulation (Figure 2.3(a), 2.3(b)).

To further validate the observation that Mst1 is not a component of the integrin outside-in pathway (Figure 2.4(a), 2.4(b)), we compared the ability of wt and Mst1$^{h/h}$T cells to migrate across transwells coated with ICAM-1. As expected, the presence of ICAM-1 readily and strongly enhanced CCL19-induced chemotaxis of wt CD4 T cells (Figure 2.4(c)). LFA-1 engagement

especially promoted migration of wt T cells through 3 μm pores, which are less than half the cells diameter. This is consistent with the observation that migration through 3 μm pores is particularly dependent on myosin-mediated contractility and is facilitated by integrins [101] .

Interestingly, ICAM-1 enhanced migration of Mst1$^{h/h}$ T cells through 5 μm pores in response to CCL19 (Figure 2.4(c)). This is likely due to the ability of ICAM-1 to induce LFA-1-dependent polarization of Mst1$^{h/h}$ T cells (Fig. 2C, D). However, ICAM-1 was unable to promote CCL19-induced migration through 3 μm pores compared to chemokine-free, ICAM-1 only controls (Figure 2.4(c)). These findings indicate that LFA-1 outside-in signaling can partially compensate for Mst1 deficiency in promoting T cell migration through non-constraining pores; however, there is a strict requirement for Mst1 in T cell migration that requires cellular contractility.

2.3.5 Mst1 regulates Myosin IIa localization

To determine how Mst1 regulates cellular contractility, we performed live differential interference contrast (DIC) imaging of wt and Mst1$^{h/h}$ CD4 T cells migrating on ICAM-1-coated surfaces. Over time, a fraction of Mst1$^{h/h}$ CD4 T cells but no wt cells formed long uropods. These elongated cells represent a subpopulation of Mst1$^{h/h}$ CD4 T cells with severe defects in contraction, similar in scale to pharmacologic inhibition of ROCK, an activator of Myosin IIa at the trailing edge [101]. To investigate Myosin IIa directly, we used confocal

microscopy to visualize the localization of Myosin IIa-GFP fusion protein and F-actin by staining migrating wt and Mst1$^{h/h}$ CD4 T cells with phalloidin. Three-dimensional reconstruction of z-axis serial confocal micrographs of wt CD4 T cells allowed us to visualize the lamellipodia, the lamellae with dorsal and lateral membrane ruffles, the trailing edge of the membrane contacting the substratum, and the upwards-pointing uropod. While F-actin is sparse in the uropod, Myosin IIa is particularly enriched in the membrane extending from the trailing edge towards and into the uropod of wt cells (Figure 2.5(a)). Myosin IIa co-localized with the actin cytoskeleton at sites of membrane ruffling and at the trailing edge (Figure 2.5(a), 2.5(b)). Three-dimensional reconstruction of Mst1$^{h/h}$ CD4 T cell images revealed several abnormalities. The leading edge of Mst1$^{h/h}$ CD4 T cells did not form a classic fan-like lamellipodium. Membrane ruffles were observed in the leading edge rather than in the dorsal lamellae (Figure 2.5(a)). Similar to wt cells, Myosin IIa co-localized with F-actin in the trailing edge. However, instead of extending predominantly into the uropod, Myosin IIa was diffusely localized throughout the mid-body and lamellae of Mst1$^{h/h}$ CD4 T cells (Figure 2.5(a), 2.5(b)). The dynamics of Myosin IIa-GFP were also assessed by live TIRF imaging to visualize Myosin IIa near the ventral membrane that contacts the substratum. In wt T cells, Myosin IIa clusters were sparsely observed in the mid-body but enriched in the posterior membrane during migration (Figure 2.5(b)). Although Myosin IIa clusters were observed in the posterior membrane of Mst1$^{h/h}$ T cells, it

was also present in the mid-body and extended into multipolar anterior protrusions (Figure 2.5(b)). These data indicate that Myosin IIa localization was dysregulated in the absence of Mst1, resulting in a defect in T-cell contraction, consistent with a lack of migration in 3μm pore transmigration assay.

2.3.6 Mst1-dependent Myosin IIa activity controls the spatial distribution of low and higher affinity LFA-1

Myosin IIa contraction regulates LFA-1 adhesion and de-adhesion [32, 91, 101]. Different affinity LFA-1 conformations are spatially segregated within the membrane of migrating T cells. Affinity-specific antibodies have revealed that LFA-1 molecules at the leading edge and mid-body are in the intermediate and high affinity conformations respectively while uropodal and trailing edge LFA-1 molecules are of low affinity [33, 34, 89]. To determine if the mis-localization of Myosin IIa observed in Mst1-deficient cells affects the distribution of different affinity LFA-1 molecules, wt and Mst1$^{h/h}$ CD4 T cells were stained with the antibody clone 2D7, which recognizes low affinity LFA-1 [102]. As previously published, low affinity LFA-1 was restricted to the trailing edge of wt CD4 T cells (Figure 2.5(c), 2.5(d)). Unfortunately, antibodies that specifically recognize intermediate and high affinity LFA-1 are unavailable for mouse cells. However, co-staining T cells with limiting amounts of the pan-affinity specific LFA-1 antibody, M17/4 together with 2D7 allowed preferential detection of higher (intermediate and high) affinity LFA-1 by M17/4 (Figure

2.5(c), 2.5(d)). Dual staining with M17/4 and 2D7 revealed that wt cells showed enriched distribution of higher affinity LFA-1 in the mid-body behind the leading edge (Figure 2.5(c), 2.5(d)). In contrast, in many Mst1$^{h/h}$ CD4 T cells, low affinity LFA-1 was distributed inappropriately to the lamellae, an actin-rich region behind the leading edge. Moreover, a considerable number of Mst1$^{h/h}$ CD4 T cells generated two leading edge protrusions, with both lamellae containing mis-localized low affinity LFA-1 (Figure 2.5(d), 2.5(e)). Higher affinity LFA-1 was also mis-localized in multipolar cells, generally to the leading or trailing edges. Thus, we conclude that loss of Mst1 disrupts the spatial organization of low and higher affinity LFA-1 and suggest that this defect significantly contributes to the well-established adhesion defects observed of Mst1deficient T cells [52, 76].

To determine whether inhibition of Myosin IIa activity phenocopies the mis-localization of low affinity LFA-1 in Mst1$^{h/h}$ cells, wt CD4 T cells were treated with Blebbistatin, an inhibitor of myosin ATPase activity [103]. Indeed, Blebbistatin-treated wt cells exhibited broad distribution of low affinity LFA-1 and could form two leading edges similar to Mst1$^{h/h}$ CD4 T cells (Figure 2.5(e), 2.5(f)). Together, these data support a novel regulatory role for Mst1 in coordinating Myosin IIa contractility to facilitate the appropriate distribution of low and higher affinity integrins during T cell migration.

2.3.7 Mst1 interacts with and phosphorylates Myosin Light Chain (MRLC2) at Thr10/11

To determine how Mst1 regulates myosin function, we asked whether Mst1 can phosphorylate MRLC2. MRLC2 is classically phosphorylated at Thr18 and Ser19 by myosin-light chain kinase (MLCK) and Rho-kinase (ROCK), to induce contraction by myosin II [66]. In order to determine whether Mst1 phosphorylates MRLC2 at these two sites, we fixed both wildtype and $Mst1^{h/h}$ T-cells that are migrating on ICAM-1 in the presence of CCL19 and intracellularly stained with specific antibody for phosphorylation at both sites. MRLC phosphorylated at Thr18 and Ser19 localized between uropod and mid-body, especially where cells were elongated (Figure 2.6(a)). This observation is consistent with the function of activated myosin in providing contraction between cell body and trailing edge in order to detach the adhesive tail [32,40,66,67,91]. Interestingly, $Mst1^{h/h}$ T-cells with the antibody to a similar or mildly enhanced degree compared to wildtype T-cells (Figure 2.6(c)), rejecting our hypothesis that Mst1 phosphorylates MRLC2 at T19/S20.

Having determined that Mst1 did not phosphorylate MRLC2 at T19/S20, we analyzed the MRLC2 primary sequence for other potential phosphorylation sites based on a kinase consensus sequence library [104]. We found that Thr10 and Thr11 had high probability for phosphorylation by Mst1. We then carried out *in vitro* kinase assays with purified Mst1 mixed with purified recombinant

GST-MRLC2 and phosphorylation-resistant GST-MRLC2 T10/11A. We determined the level of phosphorylation by separation of recombinant proteins on an SDS-PAGE gel supplemented with Phos-tag, a chemical that retards phosphorylated proteins' mobility [105], and found two phosphorylation sites (Figure 2.6(c)), both of which were completely abrogated in the GST-MRLC2 T10/11A. This result indicated that Mst1 can phosphorylate MRLC2 at both T10 and T11.

Given the result of kinase assay, we wanted to examine the ability of Mst1 and MRLC2 intracellularly. Due to common difficulties in performing kinase-substrate immunoprecipitation, we decided to use luciferase complementation [106], an assay that allows sensitive detection of weak protein-protein interactions. We fused Mst1 kinase domain to the N lobe of luciferase (Mst1-N-Luc) and MRLC2 to the C lobe (MRLC2-C-Luc) and co-transfected them into 293T cells. Extensive bioluminence in the presence of luciferin as compared to Mst1-N-Luc with unfused C-Luc which had only slight background signal (Figure 2.6(d)). This result confirmed the intracellular interaction of Mst1 and MRLC2.

Overall, these results clearly indicated that Mst1 not only interacts with but also phosphorylates MRLC2 at T10/11 but not T19/S20.

2.4 DISCUSSION

Together, our data demonstrates that Mst1 regulates T cell polarization and promotes progressive integrin-dependent T cell migration through control of Myosin IIa activity. Visualization of Myosin IIa and F-actin localization using confocal and TIRF microscopy allowed us to identify a role for Mst1 in restricting Myosin IIa localization to dorsal membrane ruffles, the trailing edge membrane, and the uropod. Moreover, we show that Myosin IIa regulates the spatial distribution of low and high affinity LFA-1 in migrating T cells. Mst1 deficiency or Myosin II inhibition resulted in the establishment of multipolar cells, elongated uropods and deregulated localization of low affinity LFA-1.

Precise control of contraction is mediated by phosphorylation of multiple sites within both Myosin light and heavy chains [90]. Normal levels of di-phosphorylated-Myosin Light Chain (MRLC2-T18S19) in $Mst1^{h/h}$ T cells suggest that Mst1 is not required to regulate MRLC2 at these sites. However, we identified MRLC T10/T11 to be phosphorylated by Mst1 kinase.

Another possible mechanism is if Mst1 controls LFA-1 anchoring to the actinomyosin network. LFA-1 association with the actin cytoskeleton is via binding to Talin [107] and coincides with association of LFA-1 with Myosin IIa [32]. Talins are recruited to the CD18 cytoplasmic domain of LFA-1 by RIAM, an adapter protein that associates with Kindlin and Mst1 [107]. It will be important in future studies to assess the necessity for Mst1 kinase

activity or adapter function in RIAM-dependent anchoring of LFA-1 to the actin cytoskeleton. While multiple components of the focal adhesion complex can be phosphorylated [108], it remains to be determined whether any are Mst1 substrates and how phosphorylation affects integrin association with the actinomyosin network.

Myosin IIa-mediated contraction is also required for antigen-dependent responses. Although interstitial migration in the lymph node is integrin-independent [109], T cells rely on Myosin IIa-dependent contraction to squeeze through narrow gaps [66, 110]. As they migrate, they form transient immune kinapses with antigen presenting cells [111]. Upon high affinity binding between the T cell receptor and its cognate peptide-MHC antigen, a stable, long lasting immune synapse forms. The immune synapse is spatially organized into concentric regions with TCRs accumulating in the central supramolecular activation cluster (cSMAC) surrounded by LFA-1 in the peripheral SMAC. LFA-1 recruitment to the pSMAC and subsequent delivery of the microtubule organizing center (MTOC) to the synapse are dependent on Myosin IIa [112, 113]. While much is known about MTOC delivery [114], it less clear how Myosin delivers LFA-1 to the pSMAC. Interestingly, Mst1 is activated following TCR stimulation [47] and is required for stable immune synapse formation [52]. It remains to be determined if LFA-1 recruitment to the pSMAC is also regulated by Mst1-directed Myosin IIa activity.

Myosin contractility is regulated by myosin regulatory light chain (MRLC2) in non-myocytes. In turn, MRLC2 is regulated via phosphorylation. There are several sites shown to be phosphorylated on MRLC2 [115]. Phosphorylation of T18/S19 has been well characterized to activate myosin contractility [101,115]. We have identified another pair of sites at Thr10/11 phosphorylated by Mst1 kinase. Beach *et al* determined that in HeLa cells Thr10 phosphorylation did not seem to have physiological importance [115]. However, this phosphorylation pair may be required for myosin activation or localization in T-cells, which exhibit a completely different migratory pattern than HeLa cells.

In summary, we have identified a new requirement for Myosin IIa in controlling the spatial distribution of low and high affinity LFA-1 and have demonstrated a requirement for Mst1 in controlling Myosin IIa localization and activity during T cell migration. By advancing our insight into the molecular mechanisms controlling integrin function, T cell contractility, polarization and migration, our findings help to elucidate the distinct cellular defects that cause the primary immunodeficiency resulting from Mst1 dysfunction.

2.5 FIGURES

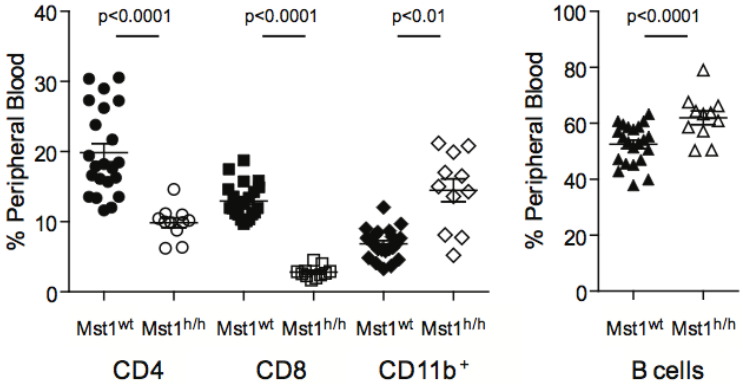

(a)

Animal	74522	103912	109123	113385	93422	88450	84145	93422	93421
Phenotype	*WeeT*	*WeeT*	*WeeT*	*WeeT*	Normal	Normal	Normal	Normal	Normal
SNP assays									
02.162.380	B	H	B	B	H	H	B	H	H
02.164.067	B	H	B	B	H	H	B	H	H
02.168.176	B	B	B	B	H	H	B	H	H
02.170.634	B	B	B	B	H	H	H	H	H
02.171.634	B	B	H	B	H	B	H	H	H
02.171.836	B	B	H	B	H	B	H	H	H
02.172.743	B	B	H	B	B	B	H	B	H
02.175.882	H	B	H	B	B	B	H	B	H
02.176.046	H	B	H	B	B	B	H	B	H

(b)

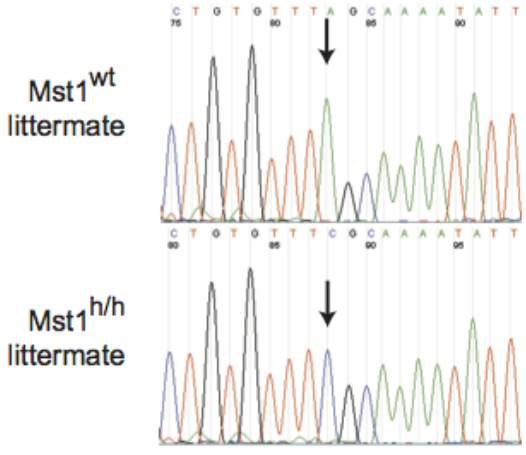

(c)

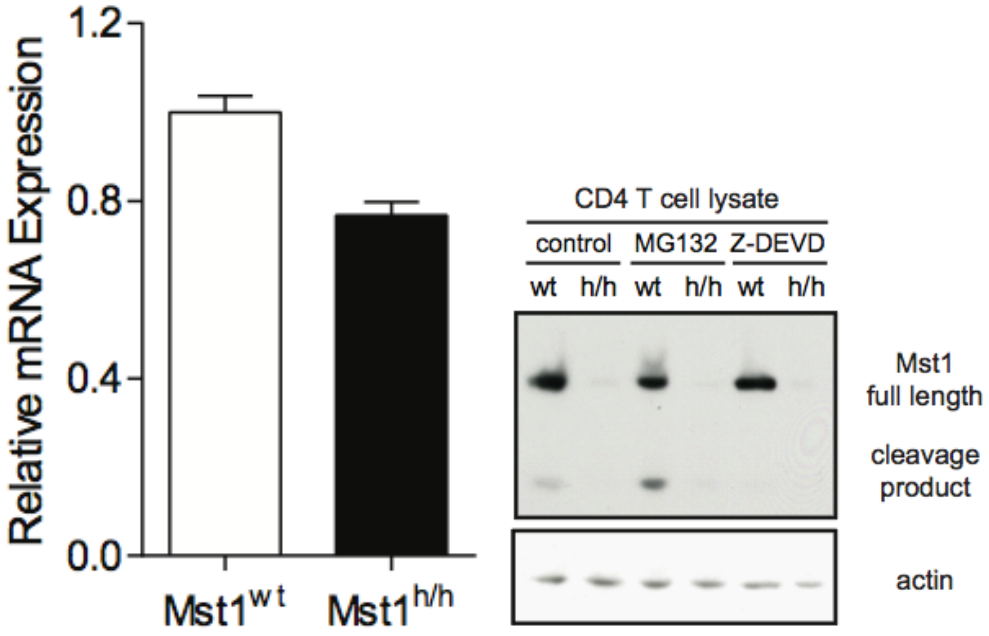

(d) (e)

Figure 2.1. Point mutation in Mst1 kinase results in degradation of Mst1 protein , resulting in decreased peripheral T-cells in $Mst^{h/h}$ mice. **(A)** Representation of CD4 and CD8 T cells, CD11b+ and B cells in the peripheral blood of wt and $Mst^{h/h}$ mice. **(B)** Inheritance of homozygous C57BL/6 (B), 129Sv/ImJ (C) or heterozygous (H) SNPs in F2 mice generated by crossing Mst1h/h mice from the original C57BL/6 background to 129Sv/ImJ. Genetic mapping of T-lymphopenic (WeeT) and normal mice isolated a 4.5 Mb region on chromosome 2 harboring the causative mutation. **(C)** $Mst^{h/h}$ mice harbor an A to C transversion in exon 5 of the Mst1 gene, resulting in change of Leu157 within the Mst1 kinase C-lobe to Arg (L157R). **(D)** Similar abundance of Mst1 transcripts in wt and $Mst^{h/h}$ T cells. **(E)** Mst1h/h T cells have reduced Mst1 protein levels in the presence or absence of proteosome (MG132) or caspase-3 inhibitors (Z-DEVD).

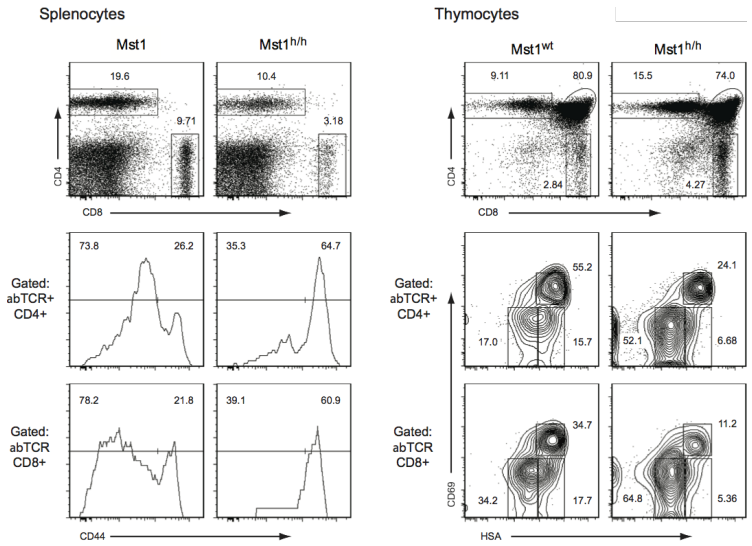
Splenocytes
Thymocytes
Mst1
Mst1h/h
Mst1wt
Mst1h/h
19.6
9.71
10.4
3.18
9.11
80.9
2.84
15.5
74.0
4.27
CD4
CD8
Gated: abTCR+ CD4+
73.8
26.2
35.3
64.7
55.2
17.0
15.7
24.1
52.1
6.68
Gated: abTCR CD8+
78.2
21.8
39.1
60.9
34.7
34.2
17.7
11.2
64.8
5.36
CD44
CD69
HSA

(a)

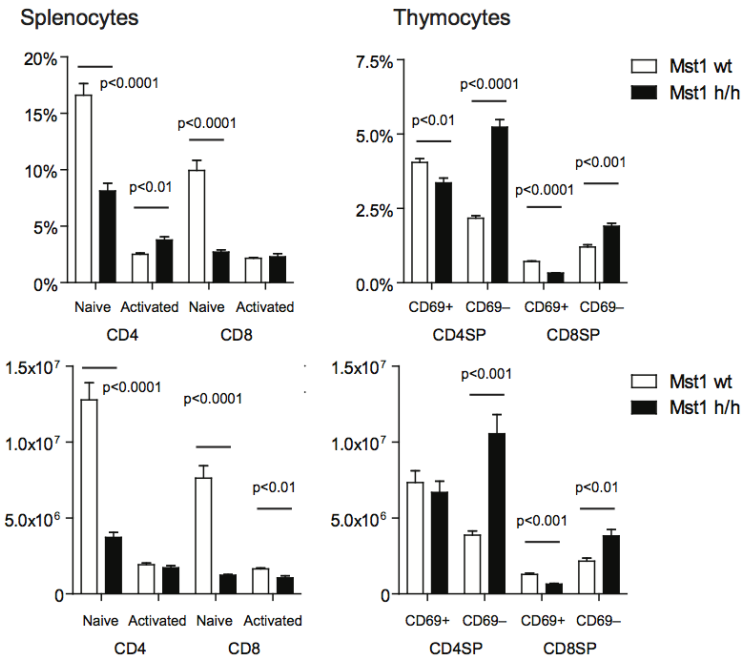
Splenocytes
Thymocytes
Mst1 wt
Mst1 h/h
20%
15%
10%
5%
0%
p<0.0001
p<0.01
p<0.0001
Naive
Activated
Naive
Activated
CD4
CD8
7.5%
5.0%
2.5%
0.0%
p<0.01
p<0.0001
p<0.0001
p<0.001
CD69+
CD69–
CD69+
CD69–
CD4SP
CD8SP
1.5x10^7
1.0x10^7
5.0x10^6
0
p<0.0001
p<0.0001
p<0.01
p<0.001
p<0.001
p<0.01

(b)

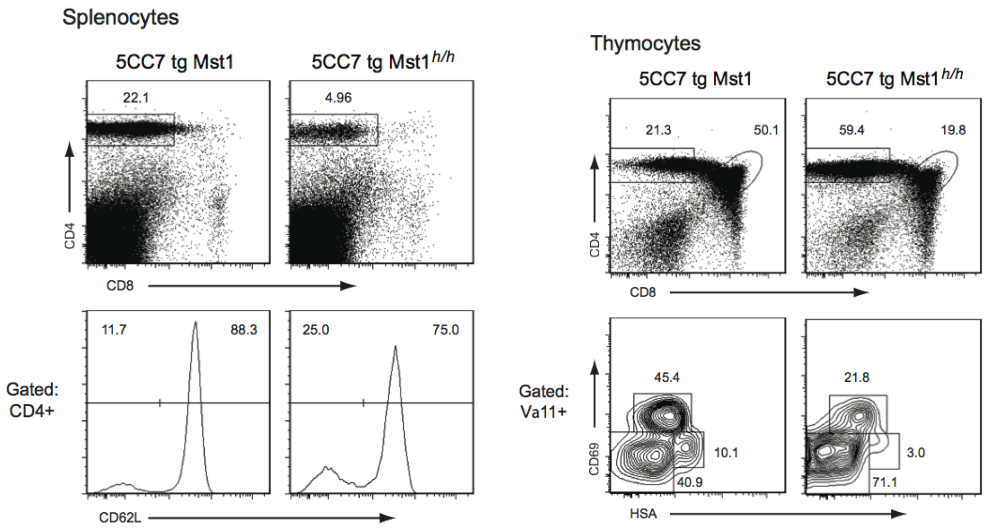

(c) (d)

Figure 2.2. Reduced naive peripheral T cells and increased mature thymocytes in Mst1h/h mice.**(A)** Representation and **(B)** total cell numbers of splenic naive ($CD44^{low}$) and effector/memory ($CD44^{hi}$) T cells and thymic populations. CD4SP and CD8SP thymocytes expressing high levels of $\alpha\beta$TCR were further analyzed for maturity based on differential expression of CD69 and HSA. Less mature SP thymocytes were $HSA^{+}CD69^{+}$, while more mature thymocytes were $HSA^{low}CD69^{neg}$. **(C)**Splenic 5CC7 TCR transgenic T cells were assessed for prior activation on CD62L expression. **(D)** Thymic profiles of wt and Mst1h/h 5CC7 TCR tg mice including delineation of less mature ($HSA^{+}CD69^{+}$) and more mature ($HSA^{low}CD69^{neg}$ clonotypic CD4SP thymocytes.

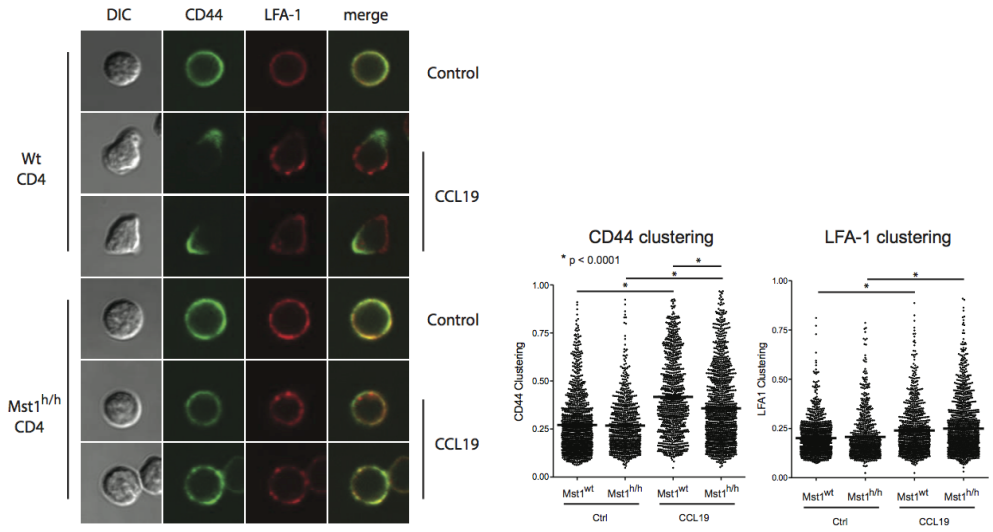

(a) (b)

Figure 2.3. Impaired polarization but not LFA-1 clustering in Mst$^{h/h}$ T-cells **(A)** Wt and Mst$^{h/h}$ CD4 T cells were stimulated with 100 ng/mL CCL19 in PBS. Polarization of CD44 to the uropod and LFA-1 distribution were visualized by confocal microscopy. **(B)** Computational scoring of CD44 and LFA-1 clustering on wt and Mst$^{h/h}$ CD4 T stimulated with 100 ng/mL CCL19 in PBS prior to fixation and staining for LFA-1 and CD44 expression.

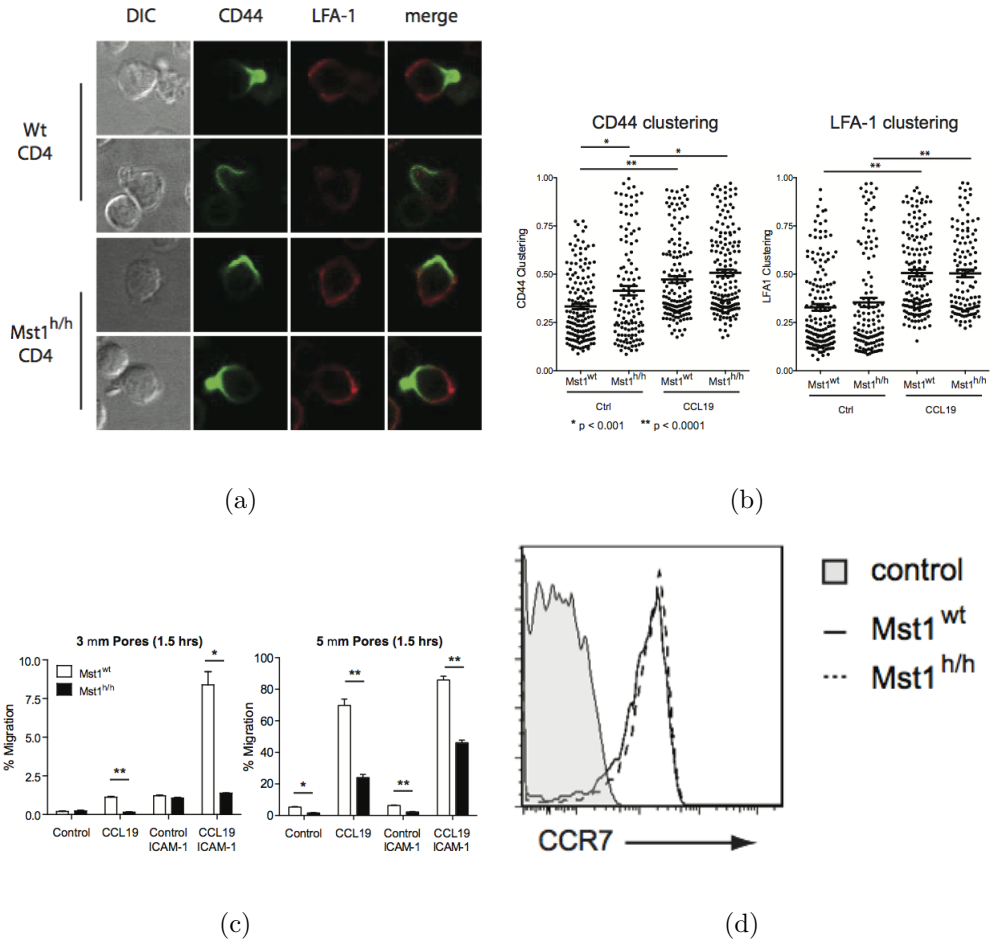

Figure 2.4. Outside-in integrin signaling rescues polarization but not migration defects in Mst$^{h/h}$ T-cells **(A)** Wt and Mst$^{h/h}$ CD4 T cells were seeded into slide chambers pre-coated with 100 ng/mL ICAM-1-Fc prior to stimulation with CCL19. Polarization of CD44 to the uropod in comparison to LFA-1 expression was visualized by confocal microscopy. **(B)** Computational scoring of CD44 and LFA-1 clustering during live imaging of wt and Mst$^{h/h}$ CD4 T cells on ICAM-1 coated chamberslides stimulated with 100 ng/mL CCL19 in presence of 0.08 ng/mL Alexa647-anti-CD11a/LFA-1 (M17/4) and Alexa488-anti-CD44. For each time point, 99-166 individual cells were analyzed for receptor clustering. **(C)** Transmigration of purified wt and Mst$^{h/h}$ CD4 T cells in response to 100 ng/mL CCL19 through 3 μm or 5 μm pores pre-coated with BSA or ICAM-1 Fc. Data is displayed as mean ± SEM of triplicate samples in a single experiment representative of 3-5 independent experiments. **(D)** Cytometric analysis of wt and Mst$^{h/h}$ CD4 T cells stained for CCR7.

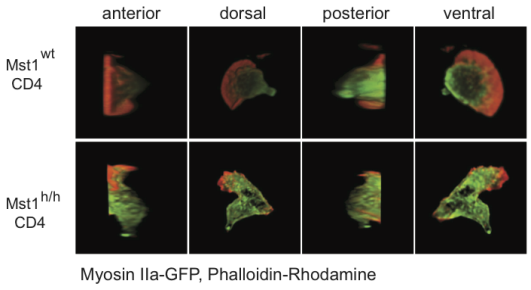
anterior
dorsal
posterior
ventral
Mst1 wt CD4
Mst1 h/h CD4
Myosin IIa-GFP, Phalloidin-Rhodamine

(a)

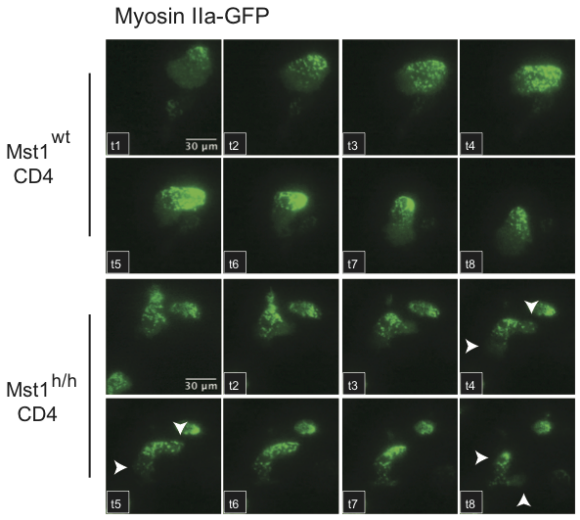
Myosin IIa-GFP
Mst1 wt CD4
Mst1 h/h CD4
t1
t2
t3
t4
t5
t6
t7
t8
30 µm

(b)

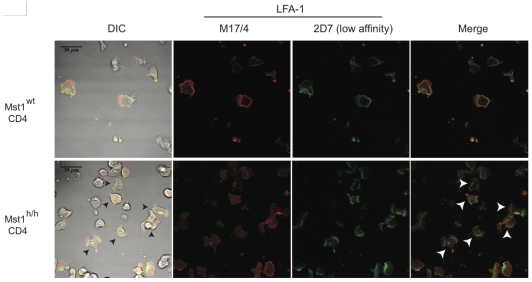
LFA-1
DIC
M17/4
2D7 (low affinity)
Merge
Mst1 wt CD4
Mst1 h/h CD4

(c)

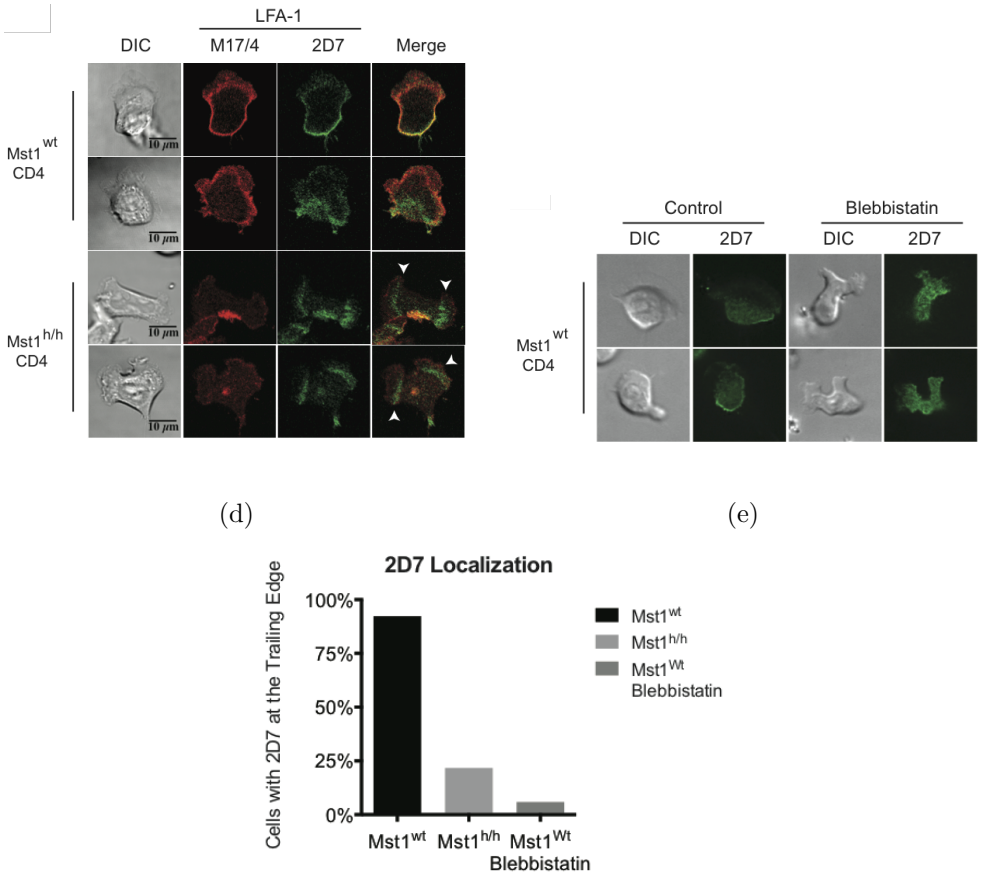

Figure 2.5. Mst1 and myosin together control low affinity integrin localization in Mst$^{h/h}$ T-cells **(A,B)** Wt and Mst1h/h CD4 T cells expressing Myosin IIa-GFP were seeded into slide chambers pre-coated with 1 μg/mL ICAM-1-Fc and stimulated with CCL19 prior to fixation and staining of F-actin with Rhodamine-phalloidin. **(A)** Three-dimensional image reconstruction from z-stacks of confocal micrographs. **(B)** Wt and Mst$^{h/h}$ CD4 T cells expressing Myosin IIa-GFP were visualized by live TIRF microscopy. Arrows indicate bipolar morphology. **(C,D)**Wt and Mst1h/h CD4 T cells were stimulated as above and stained with 2D7 (anti-low affinity CD11a/LFA-1, green) and M17/4 (anti-CD11a/LFA-1, red) **(E)** Wt CD4 T cells stimulated as above with or without Blebbistatin treatment were stained with 2D7 and visualized by immunofluorescence. **(F)** Quantification of data from **(E)**.

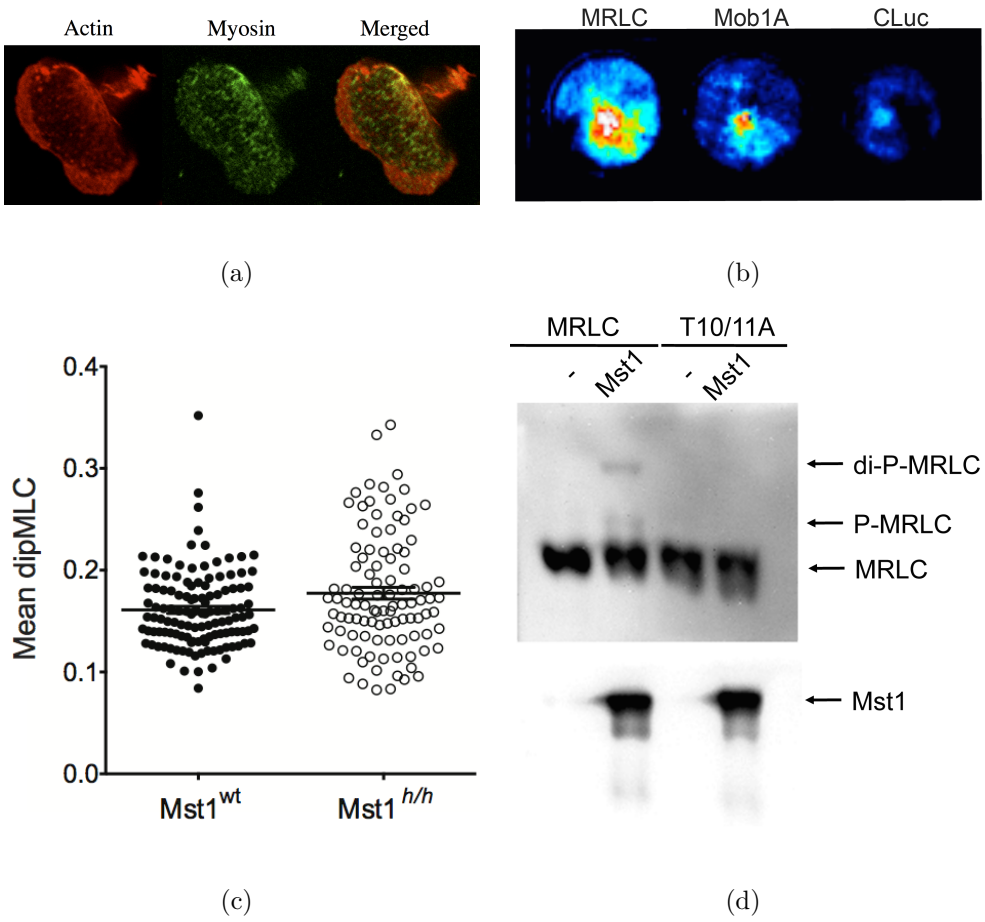

Figure 2.6. Mst1 interacts with and phosphorylates MRLC2 at Thr10 and Thr11 **(A)**T18/S19 phosphorylated myosin light chain staining of CCL19 stimulated T-cells migrating on ICAM-1-coated coverslips. **(B)** Luciferase complementation assay of 293T cells transfected with Mst1-N-Luc and MRLC2-CLuc, Mob1A-CLuc, or CLuc by itself. Signal was detected with IVIS 200 in vivo imaging system. **(C)**Levels of T18/S19-phosphorylated Myosin Light Chain determined by analyzing fluorescent micrographs of wt and $Mst1^{h/h}$ CD4 T cells stimulated with CCL19 in ICAM-1 coated chamber slides. **(D)** *In vitro* kinase assay with purified flag or GST recombinant proteins. Either Mst1 or null control was mixed with GST-tagged wt MRLC2 or T10/11A mutant MRLC2, supplemented with 100μM ATP for kinase reaction. Differentially phosphorylated protein was separated from un-phosphorylated form on an SDS-PAGE gel with Phos-tag. MRLC2 bands were detected with anti-MRLC2 antibody. Mst1 bands were detected with anti-flag antibody.

3. Triple Functions of L-plastin in Regulating T-Lymphocyte Egress and Migration

L-plastin is a filamentous (F-) actin bundling protein. It has been shown to be localized to T-cell lamellipodia and important for thymocyte egress and T-lymphocyte migration. However, the detailed molecular function of L-plastin in T-cell migration has never been thoroughly investigated. This study reveals two functions of L-plastin in promoting T-lymphocyte migration: facilitating formation of lamellipodium, and promoting the formation of microadhesion at contact zone. During this investigation, we have for the first time discovered a novel F-actin-rich L-plastin dependent microadhesion structure in T-lymphocytes. We have also identified a new pathway in which Mst1 kinase phosphorylates L-plastin threonine-89, a modification required for proper lamellipodium organization. Finally, wildtype but not Thr89Ala mutant can rescue L-plastin dependent thymocyte egress *in vivo*.

3.1 INTRODUCTION

T-cells develop in thymus, a primary lymphoid organ in mammals. Upon completion of intrathymic development, $CD69^{low}HSA^{low}$ and Sphingosine 1-Phosphate Receptor 1($S1PR1^{high}$) mature thymocytes are ready to emigrate from thymus via reverse extravasation across vascular endothelium into peripheral blood and secondary lymphoid organs (reviewed in [116]). Various genetic deficienies lead to accumulation of mature thymocytes inside thymus and concurrent decrease in the number of mature T-cells in periphery. These models include Mst1 kinase knockout and L-plastin knockout mice.

Mst1 kinase has been demonstrated to be important for T-cell polarization, migration, integrin clustering, and Rac activation. But the phenotypes and mechanisms of various studies are not completely consistent, which leaves the question of what is the exact molecular link between Mst1 and T-cell migration defect.

L-plastin is a F-actin bundling protein with calcium binding EF-hands on its regulatory amino terminus and two actin-binding calponin-homology domains on its carboxyl terminus [117]. L-plastin knockout mice exhibit similar phenotype as Mst1 knockout mice in their inability to properly emigrate from thymus [17,118]. In addition, L-plastin KO T-cells lack lamellipodia and cannot form normal immune synapse [119, 120]. L-plastin is subject to tight control by phosphorylation. Canonical phosphorylation sites include Ser5 and

Ser7 [121–123], whose phosphorylation promotes its actin binding ability [124]. On the other hand, calcium ion binding at the N-terminal regulatory domain decreases its actin bundling capability [117].

Focal adhesions are macro-molecular complexes containing integrin, F-actin, and various signal and mechanical transducers including vinculin, paxillin, talin, α-actinin, zyxin, focal adhesion kinase (FAK) among others [28–30](reviewed in [56]). Immature focal adhesion, also known as nascent adhesion or focal complex, is transient and highly dynamic [22, 125, 126]. We speculate nascent adhesions may allow more rapid migration than mature focal adhesions. On the other hand, mature focal adhesions, interconnected and anchored through stress fibers, are highly stable structures that firmly attach cells to their substratum via integrin-ligand interactions. Actin-bundling activity is required for the formation and maturation of immature nascent adhesions whereas the indispensability of contractility is still debatable [22,125].

Mature focal adhesion-like structures have never been observed in T-cells, consistent with T-cells' rapid migration capability. In this study, we demonstrate that with high resolution total internal reflection fluorescent (TIRF) microscopy, transient and highly dynamic F-actin-rich integrin-containing microadhesions reminiscent of mesenchymal nascent adhesions can be observed. We found that microadhesion and lamellipodium formation is highly dependent on L-plastin. Consistent with previous reports [122], we also found that L-plastin may activate integrins, specifically lymphocyte function antigen-1

(LFA-1). We further demonstrated L-plastin is dependent on phosphorylation at a novel site Thr89 by Mst1 kinase. Additionally, we show that wildtype but not Thr89Ala mutant can rescue the egress defect in L-plastin-null mice. Our study suggests that L-plastin may be one of the missing molecular links between Mst1 signaling and T-cell polarity and integrin clustering.

3.2 MATERIALS AND METHODS

3.2.1 Mice

Mst1 and LPL deficient mice were generated as previously described. Mice were housed in a specific pathogen-free facility under the supervision of the Division of Comparative Medicine at Washington University School of Medicine. Animal studies were approved by the Washington University and Dartmouth College Institutional Animal Care and Use Committees.

3.2.2 Western blot analysis

CD4 T cells were purified from mouse spleen and lymph nodes with Dynabeads Untouched Mouse CD4 kit (Life Technologies, Carlsbad, CA). The purified cells were then rested at 37C for 20 minutes. Cells were then stimulated with CCL19 (100 ng 1g/mL) and lysed with Actin cytoskeleton-preserving lysis buffer (0.1% Triton X-100, 2 mM MgCl2, 150 mM KCl, 10 mM Hepes, Mini-complete phosphatase and protease inhibitors (Roche, Indianapolis, IN)), standard lysis buffer (1% Triton X-100, 150 mM NaCl, 40 mM Tris pH 7.5, Mini-complete phosphatase and protease inhibitors) or 1X NuPAGE LDS Sample buffer (Life Technologies) with reducing agent. Cell lysates were briefly spun down and separated by SDS-PAGE followed by Western blot analysis.

3.2.3 Antibodies

Antibodies used for Western blot analysis: LPL (SCBT, Dallas, Texas) and LPL-phosphoSer5 (a gift from Dr. Eric Brown), Mst1 and phospho-Thr-X-Arg (Cell Signaling Technologies, Danvers, MA), -actin (Sigma Aldrich, Saint Louis, MO). The following antibodies used for flow cytometric analysis were purchased from Biolegend (San Diego, CA) and eBioscience (San Diego, CA): anti-CD45.1-PerCPCy5.5, anti-CD45.2-Alexa700, anti-CD4-APC, anti-CD8-PECy7, anti-HSA^{-}Pacific Blue, anti-CD69^{-}PE.

3.2.4 Alignment of LPL sequences

NetPhorest (http://netphorest.info/) was used to search for potential MST phosphorylation sites computationally. Alignment of plastins was performed using ClustalW2 and Clustal Omega (http://www.ebi.ac.uk/Tools/msa/clustalo/).

3.2.5 Constructs and Cloning

The LifeAct-RFP construct was generously provided by Yunfeng Feng. Lentiviral constructs of LPL were generated with pLVX (Clontech, Mountain View, CA) as the backbone and LPL sequence amplified from pMX-LPL plasmid generously provided by Dr. Eric Brown (Genentech) with polymerase chain-reaction. Site-directed mutagenesis to generate different LPL constructs was carried out using the Quikchange kit (Stratagene, La Jolla, CA) according

to manufacturers manual. For luciferase complementation assay, Mst1 kinase domain was fused in front of the N-lobe of luciferase and LPL in back of the C-lobe of luciferase in separate constructs generously provided by Dr. David Piwnica-Worms.

3.2.6 Purification of Recombinant Protein

GST-Mst1 kinase domain, LPL protein were expressed in and purified from E. coli BL21 strain. Briefly, cells were transformed with appropriate pGEX construct and grown overnight before induction with IPTG for 1 to 3 hours. The cells were resuspended in lysis buffer (1% Triton-X 100, 1mM EDTA pH8.0, lysozyme, protease inhibitors (Roche), 50mM Tris-Base pH 8.0) and lysed with repeated freeze-and-thaw cycles in liquid nitrogen and in a 37C water bath. The lysate was subsequently sonicated to fragment bacterial DNA. GST fusion proteins were then incubated and pelleted with glutathione-beads (GE) for 6 hours and protein bound to glutathione beads were eluded with reduced glutathione (Sigma Aldrich, Saint Louis, MO) overnight.

3.2.7 *In vitro* Kinase Assay

Purified recombinant GST-Mst1 kinase domain and GST-LPL were mixed together in the presence of kinase buffer (25 mM Hepes, 10 mM MgCl2, 0.5 mM NaVO4, 0.5 mM DTT) with or without [γ-32P]-ATP. Reactions were

terminated after 45 minutes with PAGE sample buffer and boiled for 1 minute before separation by SDS-PAGE. In cases where [γ-32P]-ATP was added, the PAGE gel was stained with Coomassie Blue and visualized by autoradiography.

3.2.8 Luciferase Complementation Assay

Luciferase complementation assay was carried out as previously described. Briefly, 293T cells were co-transfected with different combinations of Mst1-N-Luc and target-C-Luc fusion constructs with FuGENE 6 (Promega, Madison, WI). One day post transfection, cells were seeded into luciferase plates. Luciferin substrate was added after 12 hours and imaged using an IVIS-200 in vivo imaging system (Caliper Life Sciences, Hopkinton MA).

3.2.9 Total Internal Reflection Fluorescence (TIRF) Microscopy

To examine microadhesion dynamics at the thin membrane-substratum interface, we used TIRF microscopy, which visualizes the 200 nm membrane region contacting the substratum/glass. CD4 T cells expressing various fluorescently-tagged proteins were allowed to settle in Leibovitz's L-15 medium supplemented with 10% fetal calf serum into Nunc Lab-Tek II chambered coverglass pre-coated for 20 minutes at 37C with 2μg/well recombinant ICAM-1-Fc (R&D Systems, Minneapolis, MN). Chamberslides were later placed into a heated and humidified chamber and imaged using MetaMorph (Molecular

Devices, Sunnyvale, CA) on a Olympus IX81-ZeroDrift 2 inverted microscope equipped with widefield fluorescence light source and shutters, celltirf TIRFM illuminator, and 490 nm, 560 nm, 640 nm laser lines. A 60X 1.49 N.A. oil objective was used to capture the images. Each channel was sequentially captured with an Andor Zyla 5.5 camera at 50 fps.

3.2.10 Generation of Bone Marrow Chimera

Hematopoietic stem cells (HSC) were purified from LPL deficient mice using the Miltenyi anti-cKit positive selection kit according to manufacturers manual, followed by fluorescence-activated cell sorting of cKit+Sca1+ cells. HSCs were subsequently allowed to proliferate in the presence of stem cell factor (50 ng/mL) and thrombopoietin (50 ng/mL) and transduced with lentivirus encoding LPL fused with green fluorescent protein. Transduced HSCs (>10,000/recipient) were injected intravenously into lethally irradiated $CD45.1^+$ congenic mice. Eight weeks following reconstitution, thymus, spleen and lymph nodes were harvested from recipients and analyzed by flow cytometry.

3.2.11 Immunofluorescent Staining of CD4 Lymphocytes

For polarity staining, purified CD4 T cells were stimulated, stained with anti-CD44-Alexa488, anti-CD11a-Alexa647 (M17/4)) and fixed with 4% paraformalde-

hyde. For actin staining, purified CD4 T cells were allowed to settle on ICAM-1 coated chamberslides and stimulated prior to fixation with 4% paraformaldehyde and permeabilization with 1% Triton X-100. Cells were then stained for filamentous actin with rhodamine-phalloidin (Life technologies) and anti-LPL specific antibody followed by anti-mouse IgG-Alexa488. Images of stained CD4 T cells were captured using an Olympus FV-1000 confocal microscope.

3.2.12 Image Processing and Analyses

Movies and images were initially processed in Fiji [127] for conversion to multichannel tiff files followed by custom Matlab programs to detect cell contour and microclusters and to compute clustering index of certain fluorescently tagged proteins. Briefly, the cell contour was detected with recursive global and local thresholding until reaching a predefined criterion. The cell contour served as the confined region for microclusters detection. Microclusters were identified by detecting local maxima, limited by size and a fraction of the total intensity of the cell. The computation of clustering index was done as previously described in Chapter 2.

3.3 RESULTS

3.3.1 Thymic egress and T-cell migration depend on L-plastin and lamellipodium formation

L-plastin (LPL) knockout mice are known to have a block in thymic egress [118], as manifested by an accumulation of both mature CD4SP and CD8SP ($CD69^{low}HSA^{low}$) thymocytes (Figure 3.1(a)). CD4 T-cells purified from $LPL^{-/-}$ mice were subjected to both Transwell assay and 2-dimensional migration on coverslips coated with the LFA-1 ligand ICAM-1 (Figure 3.1(b), 3.1(c)). Both assays confirmed that migration is dependent on LPL.

Microscopic analysis of migrating $LPL^{-/-}$ T-cells transfected with LifeAct-RFP or fixed with paraformaldehyde and subsequently stained with rhodamine-phalloidin confirmed a lamellipodial formation defect (Figure 3.1(d)) that was consistent with a previous study utilizing RNA-interference to knockdown L-plastin [119]. Since intermediate affinity LFA-1 localizes to leading edge at lamellipodium [33], the inability to extend a sizable lamellipodium is likely responsible for decreased overall migration velocity and distance observed in migration assays. On the other hand, because high affinity LFA-1 is localized to the mid-body of T-cell [33,34], forming an adhesive focal zone, mid-body of defective cells is preserved and therefore still comparably adhesive to ICAM-1 surface (Figure 3.1(d)).

These results indicated that LPL is required for efficient thymic egress, migration, and lamellipodial formation in T-cells.

3.3.2 Novel microadhesion structures in T-cells are dependent on L-plastin

In order to investigate LPL localization in rapid-migrating T-cells, LPL-GFP plasmid was transfected into wildtype T-lymphoblasts activated with anti-CD3 and anti-CD28 antibodies. Using TIRF microscopy, we observed that LPL-GFP localized to the tip of lamellipodial leading edge in T-cells migrating on ICAM-1 surface (Figure 3.2(a)). Unlike F-actin, visualized by LifeAct-RFP, which was more dynamic around the leading edge region.

In addition to lamellipodial localization, we also observed punctate structures rich in LPL-GFP in the contact zone between migrating T-cells and ICAM-1 surface (Figure 3.2(a)). Wondering whether these structures are also rich in F-actin, we visualized LifeAct-RFP in wildtype T-cells them with TIRF. Not surprisingly, F-actin colocalizes with LPL-GFP at these puncta (Figure 3.2(a)). These puncta are stable structures formed immediately behind newly formed lamellipodia and remain static relative to the substratum surface (Figure 3.2(b)), suggesting they are adhesive structures. We also noticed that the F-actin and LPL-GFP intensity is variable among different puncta in the same cells (Figure 3.2(a)). Higher content of both proteins correlates with increased local adhesion, often manifested as elongated trailing edge as cells rapidly mi-

grate, further validating the adhesive nature of these structures. Unlike the F-actin ring and integrin core associated with podosomes observed in dendritic cells and osteoclasts, F-actin localizes throughout the puncta. Hereafter, we term them "microadhesions".

To exclude the possibility of microadhesion being artefacts resulting from protein over-expression and aggregation, we fixed unmanipulated primary wild-type T-cells migrating on ICAM-1 surface and stained them with rhodamine-phalloidin. Consistent with previous observations, a side-view of phalloidin-stained cells also revealed microadhesions were confined to the bottom surface of T-cells (Figure 3.2(d), 3.2(e)).

Given the presence of LPL in the microadhesions, we asked whether LPL is required for microadhesion formation. We fixed primary wildtype and $LPL^{-/-}$ T-cells migrating on ICAM-1 surface, stained them with phalloidin, and quantified the number of microadhesions with quantitative microscopy. $LPL^{-/-}$ T-cells exhibited much fewer microadhesions both per cell and per unit area (Figure 3.2(f), 3.2(g)), suggesting that LPL is required for the formation of microadhesion.

3.3.3 Microadhesions are protein complexes of various adhesion molecules resulting from outside-in signaling

To further investigate the protein composition in microadhesions, we stained T-cells for LFA-1 or over-expressed three fluorescently-tagged proteins nor-

mally restricted to focal adhesions, including vinculin, zyxin, and talin. All three focal adhesion proteins co-localized with F-actin in microadhesions (Figure 3.3(a)). However, unlike focal adhesions [128], T-cell microadhesions did not co-localize with active myosin as detected by staining with di-phosphorylated myosin light chain. Instead, active myosin surrounds microadhesions (Figure 3.3(a)).

Next, we asked whether microadhesion formation occurred as a result of inside-out or outside-in signaling. To answer this question, we seeded T-cells either on ICAM-1-coated surface or on poly-D-lysine (PDL)-coated surface. We incubated them briefly with CCL19, a classic trigger for integrin inside-out signaling, fixed, and stained them with rhodamine-phalloidin to visualize microadhesions. We found that microadhesion formation completely depended on integrin receptor-ligand interaction since no microadhesions formed in T-cells on PDL-coated surface even in the presence of CCL19 (Figure 3.3(b)), suggesting that microadhesion formation is a result of outside-in signaling.

Microadhesions are reminiscent of highly dynamic nascent adhesions formed in sessile mesenchymal cells prior to maturation in focal adhesions [22, 126], which firmly hold the cells down to substratum. However, in T-cells, we found these microadhesions never matured into focal adhesions, or developed stress fibers. We speculates that this inability to mature ensures the rapid migration nature of T-cells. It is, however, difficult to determine whether it is the

rapid migration in T-cell that prevents microadhesion maturation or lack of maturation that leads to rapid migration.

Extravasation of T-cells occurs through specialized endothelial cells called high endothelial venules (HEV) in lymphoid organs or through activated vascular endothelial cells around inflamed tissues. To ask whether actin microadhesions form physiologically present in T-cells arrested on endothelial cells, we used fluorescent confocal microscopy to analyze T-cells migrating on top of a mono-layer of activated MS1 pancreatic endothelial cell line. We found that LifeAct-RFP-expressing T-cells arresting on MS1 cells also had microadhesions (Figure 3.4(a)), confirming microadhesions form under physiological conditions. We also fixed these cells and capture Z-series to gain the vertical details of microadhesions on MS1 cells stained for ICAM-1. Intriguingly, we found that some small actin structures extended beyond the T-cell plasma membrane into MS1 cells (Figure 3.4(b)).

3.3.4 LPL localization requires the N-terminal regulatory domain which contains a novel site for Mst1 phosphorylation

N-terminus of LPL has been shown to be important in regulation of the actin-binding activity of LPL [117, 121, 123, 124]. We asked whether the regulatory domain is also important for LPL localization. In order to test it, we transfected wildtype T-cells with a wt LPL or an LPL lacking the N-terminal 89 amino acids ($LPL_{\Delta 89}$-GFP). With TIRF microscopy, we observed

that, even in the presence of intact actin-binding domains, LPL localization to lamellipodium or actin microadhesions was disrupted (Figure 3.5(g)). This result confirms that the N-terminal regulatory domain not only governs LPL activity but also its localization.

In addition to the reported protein kinase A-dependent Ser5 phosphorylation [123], we identified a potential Mst1 kinase phosphorylation site in LPL regulatory domain with a curated online database [104]. Given the similarity of thymic egress defect phenotypes in both Mst1-deficient and LPL knockout mice, we decided to further investigate a possible regulatory link between Mst1 and LPL. Interestingly, we found that LPL gel mobility was increased in $Mst1^{h/h}$ CD4 T-cells compared with wt CD4 T-cells (Figure 3.5(c)), suggesting an altered post-translational modification. Calf intestinal phosphatase treatment equalized the band mobility of both genotypes, confirming a difference in phosphorylation (data not shown). Western blot analysis with anti-Ser5 specific antibody showed no difference in LPL Ser5 phosphorylation. To determine if Mst1 could phosphorylate the predicted site at Thr89 on LPL, we purified recombinant LPL and a Thr89Ala (T89A) mutant for *in vitro* kinase assay with purified Mst1 or its kinase dead version Lys59Arg (K59R) Mst1. Phosphorylation was detected with either ^{32}P labeling (Figure 3.5(d)) or western blot analysis with a sequence-specific anti-phospho-TXR antibody (Figure 3.5(e)). The kinase assay results showed that Mst1 indeed phosphorylates LPL at Thr89, while T89A was not phosphorylated by Mst1 (Figure 3.5(d), 3.5(e)).

Besides *in vitro* kinase assay, we wanted to confirm that Mst1 and L-plastin actually interact intracellularly. To do this, we utilized a luciferase complementation system developed in the laboratory of Dr. David Piwnica-Worms to demonstrate *in vivo* protein-protein interactions. We fused Mst1 kinase to N-lobe (Mst1-N-Luc) and LPL to C-lobe (LPL-C-Luc) of firefly luciferase. When co-expressed in 293T cells, bioluminence in the presence of luciferin can only be detected when Mst1 interacts with LPL. Significant amount of bioluminence was detected in cells expressing Mst1-N-Luc paired with LPL-C-Luc, or Mob1A-C-Luc, a well-established Mst1 substrate, but not with vimentin-C-Luc (data not shown) or C-Luc by itself (Figure 3.5(f)).

Overall, these results showed a previously unknown role for the N-terminus of LPL in directing its localization both to lamellipodium and F-actin microadhesions, as well as identified a novel threonine site at LPL residue 89 that is a target of Mst1 kinase activity.

3.3.5 Thr89 phosphorylated LPL promotes proper lamellipodial organization

Because LPL is important in both lamellipodial and microadhesion formation, we asked whether Thr89 phosphorylation regulates LPL in these two locations. We used confocal microscopy to analyze $LPL^{-/-}$ T-cells reconstituted with wildtype or phosphorylation-resistant T89A LPL-GFP, and co-stained with rhodamine-phalloidin to visualize cytoskeleton structure. Wildtype LPL

reconstituted cells were well-spread and smooth lamellipodia. Reconstituted LPL-GFP extensively localized to lamellipodia, similar to its localization in wildtype T-cells. In contrast, T89A LPL-GFP only partially reconstituted lamellipodia, and these lamellipodia had abnormal morphology. For instance, some lamellipodia exhibited regions completely devoid of F-actin, a phenotype also observed in Mst1$^{h/h}$ T-cells (Figure 3.6(c)); in other instances, there was extensive F-actin clumping at or behind the lamellipodium. Moreover, T89A LPL showed decreased localization to lamellipodium compared to wt LPL, further confirming the requirement of phosphorylation of Thr89 LPL in T-cell lamellipodia formation (Figure 3.6).

3.3.6 Phosphorylated LPL is important for LFA-1 activation and firm adhesion

Having seen a defect in lamellipodium with T89A LPL, we also asked whether it is important for microadhesion formation. We quantified the number of microadhesions in wt or T89A LPL reconstituted T-cells but found no difference in the microadhesion number. This result suggests that Mst1 phosphorylation at T89 is not required for LPL microadhesion formation. Similar to published study showing that amino acid 1-21 of LPL can activate αMβ2 integrin in polymorphonuclear neutrophils [122], we found that over-expression of LPL also activate LFA-1. Regions enriched in LPL-GFP coincided with reduced staining with 2D7, an antibody that detects low affinity LFA-1 (Figure

3.7). In addition, high LPL-GFP expressing T-cells exhibited firm adhesion at the trailing edge, resulting in reduced migration velocity, an effect not observed in cells expressing T89A-LPL-GFP (Figure 3.7(a), 3.7(b)). These results suggest that Mst1 phosphorylation of LPL T89 is required for its ability to directly and indirectly activate LFA-1 integrin. In this respect, LPL may function similarly to α-actinin and talin.

3.3.7 Wt but not phosphorylation-resistant LPL rescues T-cell egress

To determine the in vivo significance of LPL T89 phosphorylation on T cell trafficking, we evaluated the ability of re-expressing wt or T89A LPL to rescue the egress defects of $LPL^{-/-}$ T cells in bone marrow chimeras. Donor hematopoietic stem cells (HSCs) from CD45.2+ LPL-deficient mice were infected with lentivirus encoding GFP^{-}fused Wt or phosphorylation-resistant LPL (T89A) followed by injection into lethally irradiated $CD45.1^{+}$ wt mice. Eight weeks post-reconstitution, T cells derived from LPL-deficient HSCs were analyzed by flow cytometry. $GFP^{-}CD45.2^{+}$ T cells are derived from uninfected HSCs and thus lack LPL. As in non-manipulated LPL-deficient mice, GFP^{-}CD4SP and GFPCD8SP accumulated abnormally in the thymus with a specific enrichment of $CD69^{-}HSA^{-}$ mature SPs (Figure 3.8(a)). Additionally, an increase in T cells was observed in the lymph nodes, particularly the CD8 cytotoxic T cells (Figure 3.8(b)), suggesting a lymph node egress defect not previously characterized.

$GFP^+CD45.2^+$ are derived from LPL-deficient HSCs with re-expression of wt or T89A LPL. GFP^+CD4SP and GFP^+CD8SP proportions in the thymus and lymph node from wt LPL-reconstituted HSCs were reduced compared to $GFP^-CD45.2^+$ cells, indicative of rescued T cell egress (Figure 3.8(a), 3.8(b)). In contrast, GFP^+ cells expressing T89A LPL led to increased accumulation of $CD69^-HSA^-$ mature SPs in the thymus (Figure 3.8(a)). Peripheral CD4 and CD8 T cells reconstituted with T89A LPL also accumulated in the lymph nodes (GFP^+, (Figure 3.8(b)). Collectively, these results demonstrate that Mst1-mediated phosphorylation of LPL at T89 is critical for promoting normal egress and trafficking of T cells from the thymus and lymph nodes. In summary, we have demonstrated that the formation of microadhesions, actin-rich integrin-associated microclusters, in migrating T cells requires LPL. Identification of the phosphorylation of LPL by the upstream regulator Mst1 defines a novel signaling pathway, providing mechanistic insight into prior observations that both Mst1 and LPL are essential for normal T cell polarization and migration.

3.4 DISCUSSION

The organization and distribution of adhesions constitute one of the most important step in the physical process of cell migration. Cell-cell and cell-matrix adhesive structures, such as cadherin-based cell-cell junctions, cell-matrix focal adhesions, invasive podosomes have been extensively characterized [128–132]. However, to our knowledge, no similar structure has been described in migrating T-cells, even though the phenomenon of integrin-clustering at immune synapse between the T-cell and antigen presenting cells has been well characterized. Katagiri *et al* first described integrin clustering at the lamellipodia of migrating T-cells [51,52,76]. Recently, Shulman *et al* described LFA-1 dot structures in human T-cells; however, the described structures were largely devoid of F-actin or pTyr [42]. In our study, we observed extensive F-actin-rich LFA-1-positive microadhesions in T-cell-substratum contact interface with high-resolution TIRF microscopy. These dynamic but immobile structures are complexes containing F-actin, integrin, talin, vinculin, zyxin, and the actin-bundling protein L-plastin. Unlike focal adhesions, they form immediately behind newly established lamellipodia within seconds, remain stably attached to substratum, and dissolve at the trailing edge of a migrating T-cell. We also found that microadhesion formation is highly dependent on L-plastin, which is also crucial for the lamellipodium formation and integrin activation. In addition, we identified a novel Mst1 kinase-L-plastin

regulatory pathway, where L-plastin T89 regulates F-actin organization in the lamellipodium and integrin activation. *In vivo*, LPL T89 phosphorylation is required for proper T-cell thymic and lymph node egress. In summary, L-plastin has triple functions: Mst1-independent microadhesion formation, and Mst1-dependent lamellipodium formation and integrin activation.

Given the general requirement for actin anchoring of adhesion structures in other cell types and the ability of LFA-1 to associate with actin during T cell activation, it is perhaps surprising that microadhesions have not been previously appreciated in migrating T cells. A prior study of integrin dots in T cells migrating on ICAM-1-coated surfaces and endothelial cells showed no co-localization with F-actin [42, 133]. One explanation of why we are able to observe these F-actin microadhesion is that, instead of confocal microscopy, we made extensive use of TIRF microscopy, which is better equipped for observing actin structure on the membrane with minimal out-of-focus light. Confocal analysis can easily miss actin microadhesion due to out-of-focus light from the intracellular phalloidin staining. Only after we observed these structures with TIRF were we able to find the correct Z-plane on confocal microscope to visualize them clearly. We also noted that LFA-1-specific antibodies added during live imaging can block LFA-1's binding to ICAM-1 [102], preventing outside-in signaling of stained molecules, a requirement for microadhesion formation (Figure 3.8(b)).

Interestingly, stability of microadhesions directly correlated with F-actin and LPL concentrations. We have often observed that microadhesions of higher F-actin or LPL content lead to higher stability and resistance to disassembly, even at the trailing edge of a migrating cell. This resistance can drag part of the cell membrane behind and impede cell migration. We do not yet understand the mechanism that controls the size and the protein concentration of microadhesion and how it dissolves. Based on our own observation and published reports [10, 33, 34], the integrin affinity at the front edge is usually higher than at the trailing edge. The affinity of integrin within the microadhesions also likely changes in a spatially-dependent manner. Microadhesion may represent a certain way of integrin clustering, and a convenient and efficient way for bulk activation and deactivation of integrin.

We have also found that when sitting on top of activated endothelial cells, microadhesions can insert into endothelial cells, providing a possible anchor. Even though we were unable to capture whether these microadhesion can be a precursor for trans-cellular migration due to the rapid and subtle nature of these events, future studies should examine these processes. Also, close examination of T-cells fixed on top of endothelial cells showed that T-cells can insert flap-like structures (which we call "lips") into cell-cell junctions between endothelial cells. We speculate T-cell use these lips as probes for sites of diapedesis, which could be the precursor or end product of invadopodia [134].

A couple of studies have shown the importance of phosphorylated Ser5 in actin binding and bundling activity [124,135]. Phosphorylation at Thr89 is not redundant with Ser5, in that phospho-mimic T89E does not appear to bind or bundle actin better than wt or phosphorylation-resistant T89A mutant *in vivo* (data not shown). Neither did wildtype versus T89A-reconstituted $LPL^{-/-}$ T-cells show significant difference in the formation of microadhesions, which likely require intact F-actin bundling activity. However, the N-terminus as a whole is an essential regulatory part of the protein, particularly in targeting of the protein to sub-cellular locations, as evidenced by the diffuse localization of LPL lacking the first 89 residues. The particular function of Thr89 phosphorylation is more interesting. We found that T89A-reconstituted $LPL^{-/-}$ T-cells have lamellipodia with disorganized F-actin structures, which manifested as hollow lamellipodia or clumpy F-actin. Similar phenotype was also observed in $Mst1^{h/h}$ T-cells (Figure 3.6(c)). In addition, there is less accumulation of T89A LPL in lamellipodia as compared to wildtype, suggesting a potential localization problem. Finally, over-expression of wildtype but not T89A LPL results in severely immobilized T-cells. Although these T-cells have normal lamellipodia, they have heightened integrin-binding [122] and difficulty moving and deteching trailing edge [32].

The actin-binding activity of LPL can be reduced by increased association of Ca^{2+} to the two N-terminal EF hands [117]. Ca^{2+} can also indirectly regulate LPL function through the Ca^{2+} sensing protein Calmodulin (CaM).

Deletion of the putative CaM binding sequences disrupts LPL accumulation in the pSMAC of the immunological synapse, suggesting that CaM promotes LPL activity [136]. Interestingly, the LPL residues reported to bind CaM center around Thr89, the Mst1 phosphorylation site. Studies have demonstrated that PH domain binding is required for LPL function, utilized LPL deletion mutants that also disrupted T89. Therefore future studies should be conducted to dissociate Mst1 and CaM regulation of LPL. Direct evaluation of CaM binding by wt and Thr89A mutant LPL show no differences in CaM binding, indicating that the T cell egress defects of T89A are due to disruption of Mst1 phosphorylation of LPL.

We and other have clearly demonstrated that Mst1 is important for T-cell migration [52, 76, 80, 81, 87]. Mst1 is recruited from a para-nuclear location to the plasma membrane through association with RAPL, an effector of small GTPase Rap1. Two mechanisms have been proposed for how Mst1 controls migration. These include integrin clustering [52] and F-actin polymerization [80]. Studies done by Katagiri *et al* did not provide a direct molecular link between Mst1 and integrins. In addition, a B-cell line, a phenotypical normal population in Mst1 mutant mice,was used as a model to demonstrate the Mst1-dependent LFA-1 clustering. A role for Mst1 in F-actin polymerization was demonstrated by Mou *et al*, using Mst1/Mst2 double knockout thymocytes. Thymocytes are too small to be a good model to investigate actin polymerization and polarization. Additionally, the proposed molecular mechanism link-

ing Mst-dependent Mob1A/B phosphorylation to DOCK8 and Rac1 activation was completely demonstrated in the U2OS osteosarcoma cell line, which is a rather irrelevant model for T-cell biology. We, however, used primary T-cells to demonstrate LPL as a direct molecular link between Mst1 and both integrin activation and lamellipodial F-actin organization. The physiological relevance of Mst1-LPL axis was shown using bone marrow reconstitution of $LPL^{-/-}$ HSCs. The triple functions of LPL in promoting formation of the adhesion and lamellipodia resemble those of various other well-documented actin accessory proteins including myosin and α-actinin, both known to bundle F-actin and promote adhesion formation [22, 23, 29, 30, 32, 33].

In summary, we have defined a new F-actin microadhesion structures in T-cells migrating on ICAM-1 and shown actin-bundling protein L-plastin is required for the formation of these microadhesion structures, in addition to formation of lamellipodia and activation of integrin. We have also identified a regulatory pathway in which Mst1 kinase phosphorylates LPL at Thr89, a site of physiological significance in integrin activation and *in vivo* thymocyte egress. Overall, our study has provided the first concrete molecular link, L-plastin, between Mst1 and integrin clustering and activation as well as lamellipodial formation and polarization.

3.5 FIGURES

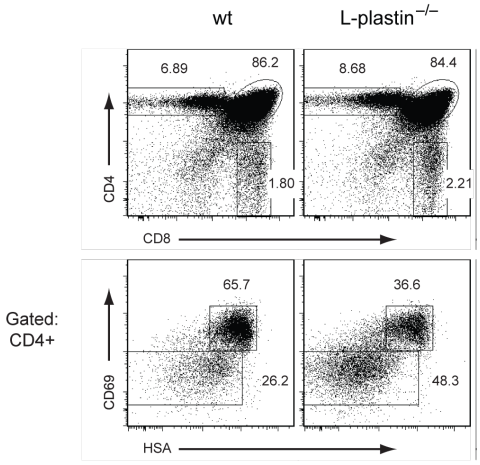

(a)

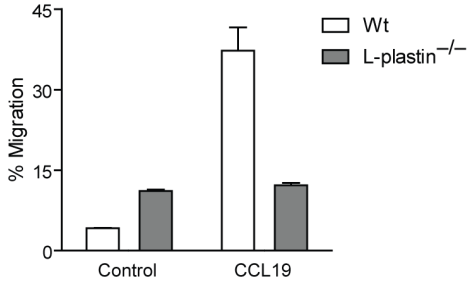

(b)

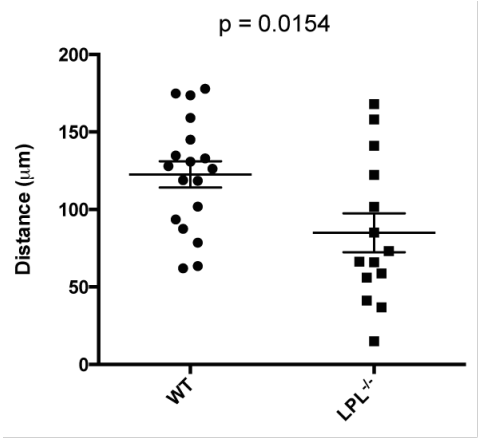

(c)

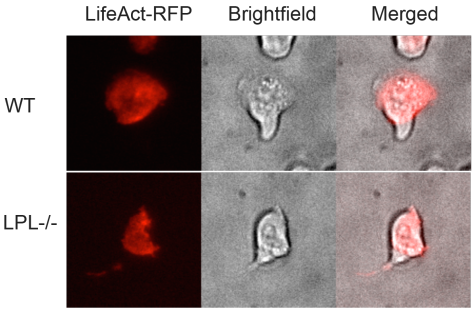

(d)

Figure 3.1. L-plastin is required for thymic egress, efficient T-cell migration, and lamellipodium formation **(A)**Flow cytometric analysis of thymocytes from wt or L-plastin$^{-/-}$ mice, stained with CD4, CD69 and HSA to distinguish mature versus immature populations. **(B)**Transwell assay of T-cells from thymocytes from wt or L-plastin$^{-/-}$ mice towards 100ng/mL CCL19 were carried out using 96 transwell inset with 5μm pores. Cells were counted after 3 hour incubation with flow cytometer.**(C)** Travel distance of purified CD4 T-cells from both genotypes migrating in the presence of 100ng/mL CCL19 on ICAM-1 coated chamberslides. Time-lapse video microscopy was used to capture migration and subsequently analyzed with chemotaxis tools in Fiji. **(D)** Purified CD4 T-cells from both genotypes were transfected with LifeAct and seeded onto ICAM-1 coated chamberslides. Photos were taken with a TIRF microscope to capture cell-matrix contact surface.

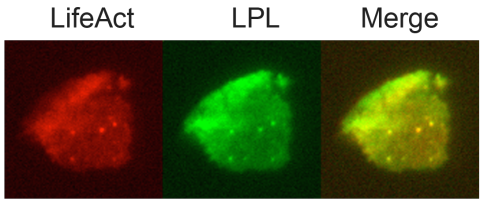
LifeAct
LPL
Merge

(a)

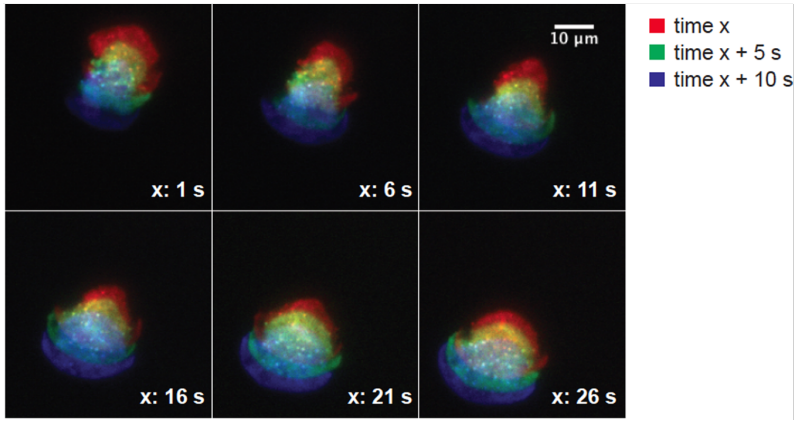
10 µm
time x
time x + 5 s
time x + 10 s
x: 1 s
x: 6 s
x: 11 s
x: 16 s
x: 21 s
x: 26 s

(b)

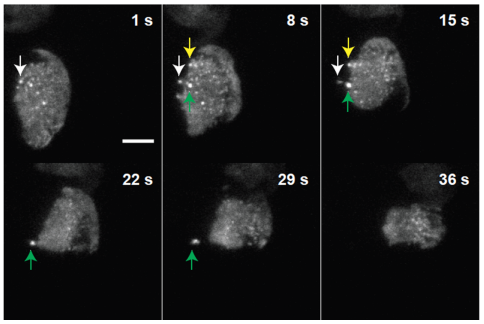
1 s
8 s
15 s
22 s
29 s
36 s

(c)

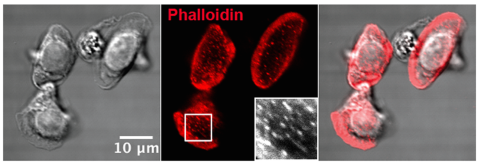
Phalloidin
10 µm

(d)

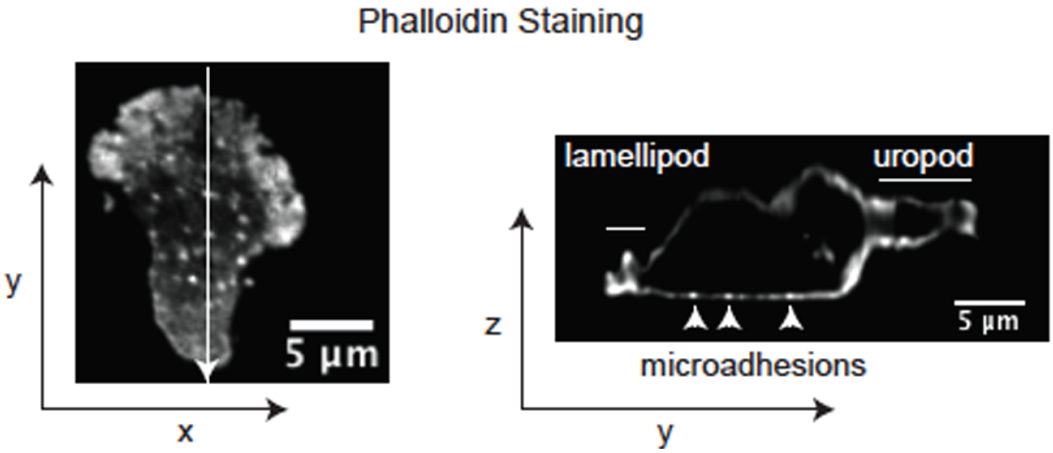
Phalloidin Staining
y
x
5 µm
lamellipod
uropod
5 µm
z
microadhesions
y

(e)

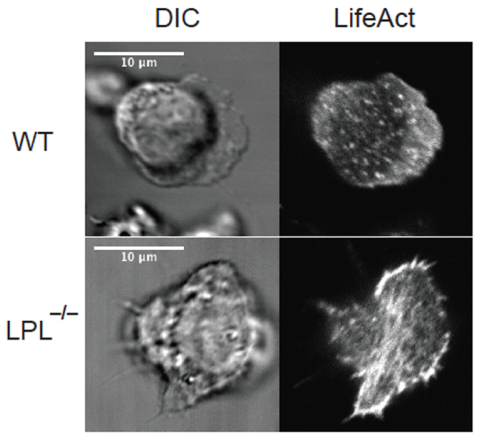
DIC
LifeAct
WT
LPL−/−
10 µm
10 µm

(f)

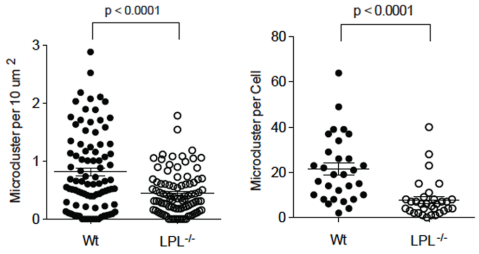
p < 0.0001
Microcluster per 10 um 2
Wt
LPL-/-
p < 0.0001
Microcluster per Cell
Wt
LPL-/-

(g)

Figure 3.2. Microadhesions are L-plastin-dependent adhesive structures **(A)**Purified wt CD4 T-cells were co-transfected with LifeAct-RFP and LPL-GFP. Photos were taken with a TIRF microscope to capture cell-matrix contact surface. **(B)**Purified CD4 T cells nucleofected with LifeAct-RFP were stimulated with CCL19 in ICAM-1 coated chamberslides and visualized by live TIRF microscopy. Three serial time points (5 seconds apart) from a single representative cell were pseudo-colored red, green and blue and then overlaid. Signal persisting in t1 and t2 appear yellow, in t2 and t3 appear aqua; in all three time points appear white. **(C)**Purified CD4 T cells nucleofected with LifeAct-RFP were visualized by live TIRF microscopy migrating on ICAM-1 coated chamberslides in response to CCL19. White, yellow and green arrows track the location of three individual actin microclusters. **(D)**Purified CD4 T cells were seeded into ICAM-1 coated chamberslides and stimulated with CCL19 (1 μg/mL) for 10 minutes followed by fixation and staining with rhodamine-phalloidin. DIC images (left) and F-actin localization (middle) were visualized by confocal microscopy. Focal actin microclusters (white dots) are readily visible in the inset corresponding to a larger view of the lower T cell. **(E)**Purified CD4 T cells were seeded into ICAM-1 coated chamberslides and stimulated with CCL19 (1 μg/mL) for 10 minutes followed by fixation and staining with rhodamine-phalloidin. F-actin localization was visualized by confocal microscopy. Focal actin microclusters (left, bottom view) are readily visible in the ventral membrane but not in the cytoplasm (right, side view) **(F, G)**Purified CD4 T cells from wt and LPL-deficient mice nucleofected with Lifeact-RFP were seeded into ICAM-1-Fc coated chamberslides. DIC images (left) and F-actin structures detected by Lifeact (right) were visualized by confocal microscopy. Microadhesions were counted and presented as number per unit area and number per cell

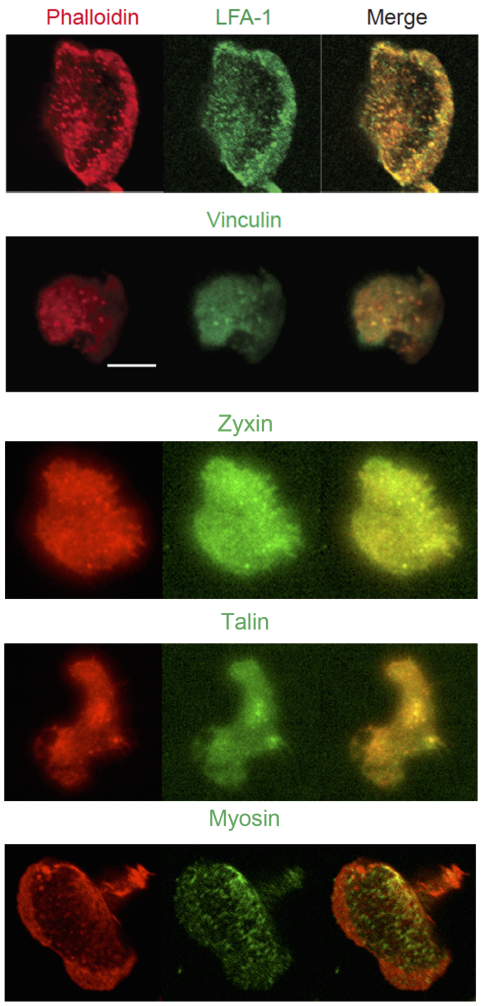

(a)

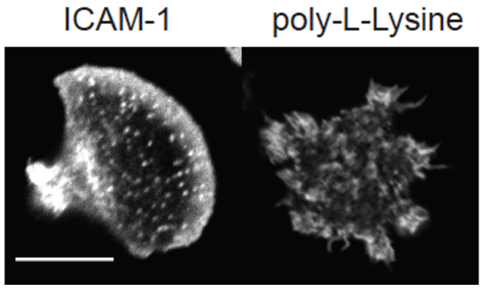

(b)

Figure 3.3. F-actin microadhesions are protein complexes containing integrin, talin, vinculin and zyxin **(A)**For LFA-1 and myosin staining, purified CD4 T cells seeded into ICAM-1-Fc coated chamberslides were fixed and stained with rhodamine-phalloidin and anti-LFA-1 antibody or permeabilized followed with anti-S18/T19 MRLC antibody. F-actin (left) and LFA-1 (right) localization at the membrane substratum interface was visualized by confocal microscopy. For others, purified CD4 T cells nucleofected with LifeAct-RFP and various protein tagged with GFP were seeded into ICAM-1-Fc coated chamberslides and visualized by live TIRF imaging. **(B)**Purified CD4 T cells seeded into poly-L-Lysine-coated or ICAM-1-Fc-coated chamberslides were fixed and stained with rhodamine-phalloidin.

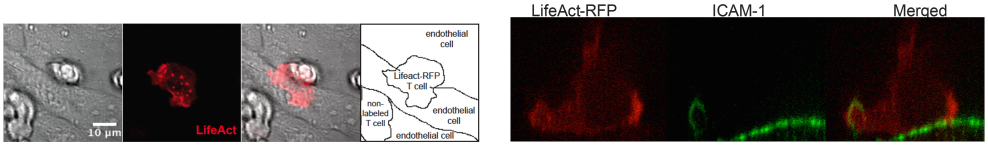

(a) (b)

Figure 3.4. F-actin microadhesions form in T-cells migrating on endothelial cells **(A,B)**Purified CD4 T cells nucleofected with LifeAct-RFP were seeded on a mono-layer of MS1 mouse endothelial cells followed by live confocal microscopy. A line diagram (right) delineates T cell and endothelial cell boundaries. A Z-stack of T-cell sitting on top of an anti-ICAM-1 stained MS1 cell was captured and a side-view is presented here (B).

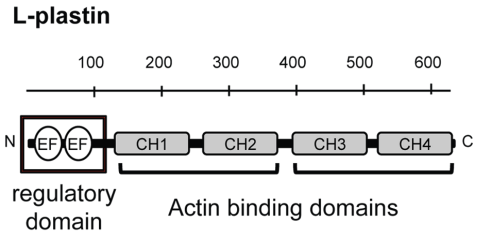
L-plastin
100
200
300
400
500
600
N
EF
EF
CH1
CH2
CH3
CH4
C
regulatory domain
Actin binding domains

(a)

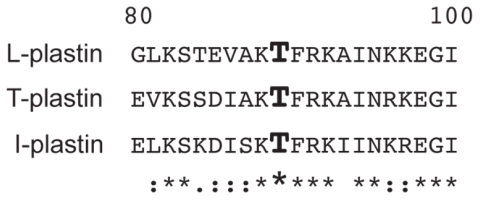
80
100
L-plastin GLKSTEVAKTFRKAINKKEGI
T-plastin EVKSSDIAKTFRKAINRKEGI
I-plastin ELKSKDISKTFRKIINKREGI
:**.:::*** **::***

(b)

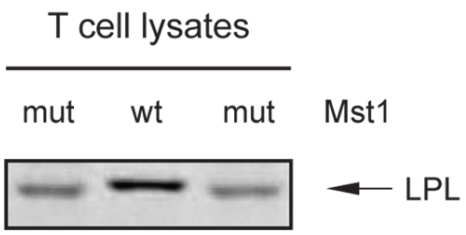
T cell lysates
mut
wt
mut
Mst1
LPL

(c)

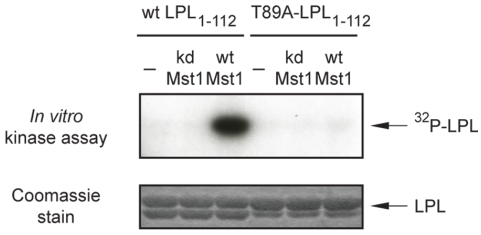
wt LPL1-112
T89A-LPL1-112
–
kd Mst1
wt Mst1
–
kd Mst1
wt Mst1
In vitro kinase assay
32P-LPL
Coomassie stain
LPL

(d)

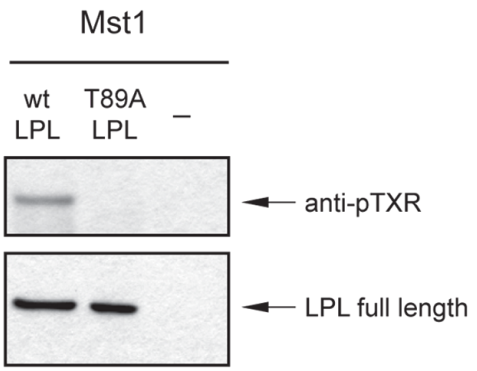
Mst1
wt LPL
T89A LPL
–
anti-pTXR
LPL full length

(e)

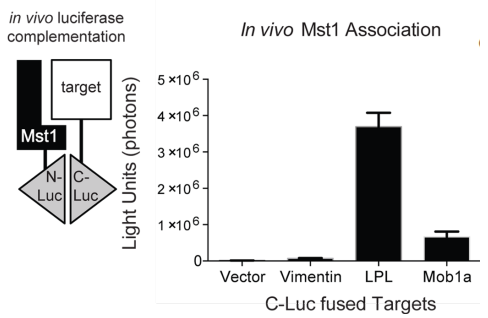
in vivo luciferase complementation
target
Mst1
N-Luc
C-Luc
In vivo Mst1 Association
Light Units (photons)
5 ×10^6
4 ×10^6
3 ×10^6
2 ×10^6
1 ×10^6
0
Vector
Vimentin
LPL
Mob1a
C-Luc fused Targets

(f)

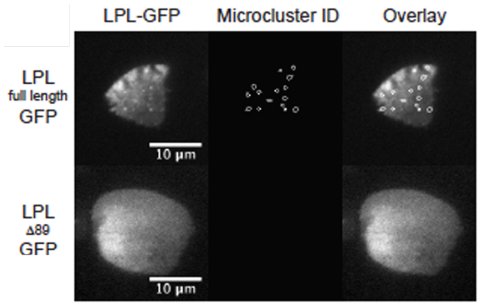

(g)

Figure 3.5. Mst1 interacts with and phosphorylates LPL at Thr89 **(A)**A schematic of LPL domains. **(B)**ClustalW2 analysis of the portion of the regulatory domain of mouse plastins containing the Mst1 phosphorylation site. **(C)**Wt and $Mst1^{h/h}$ CD4 T cell lysates were separated by SDS-PAGE. LPL gel mobility was visualized by Western blot analysis. **(D)***In vitro* phosphorylation of wt or T89A mutant LPL regulatory domain (residues 1-112) by wt or kinase defective (kd) Mst1 was visualized by autoradiography. Recombinant Mst1 and LPL input proteins were visualized by Coomassie staining. **(E)**Mst1-mediated phosphorylation of full length LPL visualized by western blot analysis with a phospho-Thr-X-Arg specific antibody. **(F)***In vivo* interactions between Mst1 and target proteins were determined by their ability to reconstitute luciferase activity. 293T cells were co-transfected with Mst1 fused to the N-terminal domain of luciferase (N-Luc) and the indicated targets fused to the C-terminal domain of luciferase (C-Luc). Empty C-Luc and vimentin-C-Luc fusion proteins, which have no reported association with Mst1, were used as negative controls. C-Luc fused to Mob1a, a known Mst1 target, was used as a positive control. **(G)**Wt LPL or LPL lacking the first 89 residues on the N- terminus were transfected into purified wt CD4 T-cells. The transfected cells were seeded onto ICAM-1 coated chamberslides. A TIRF microscope was used to visualize the LPL-GFP localization within the contact surface.

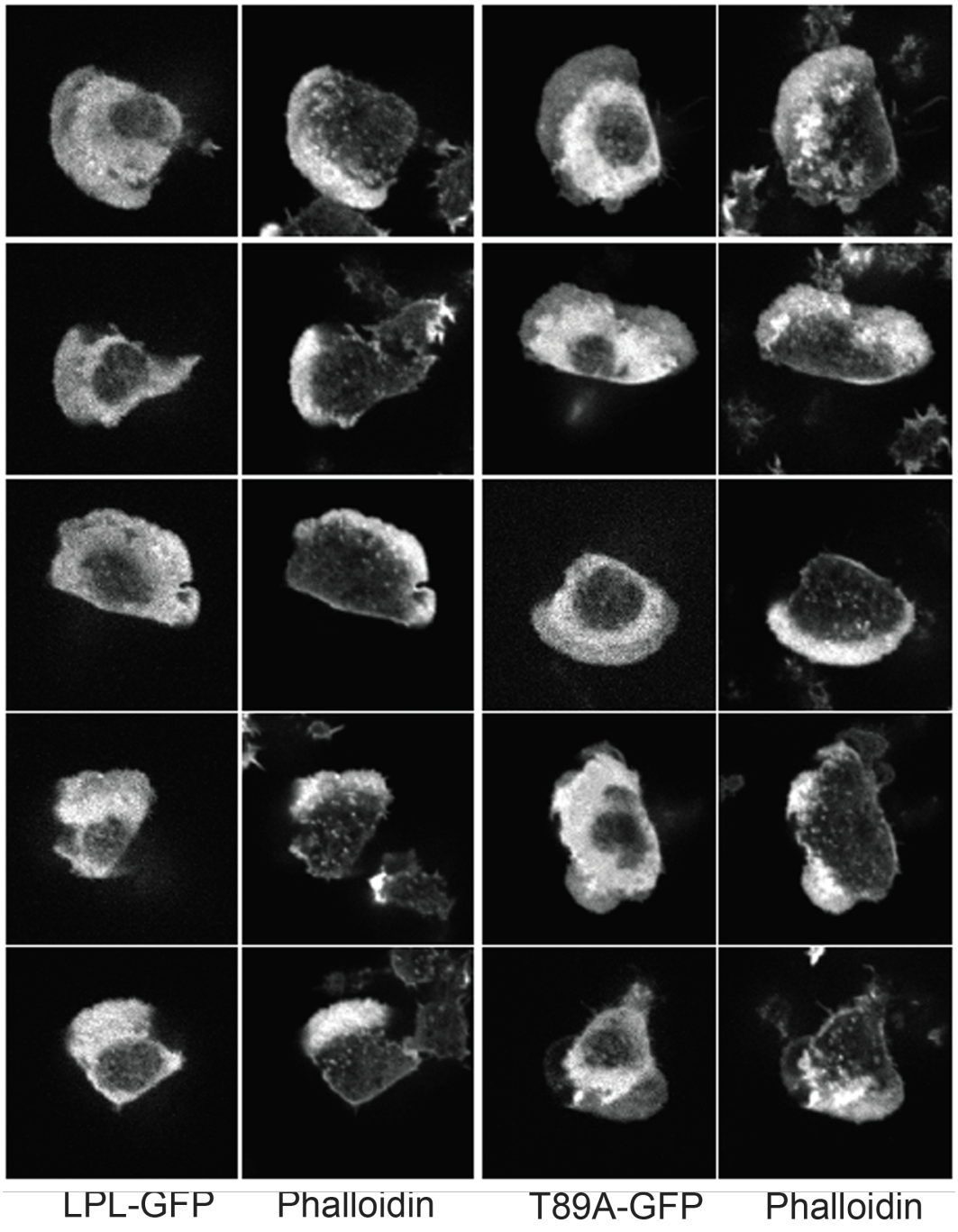

(a)

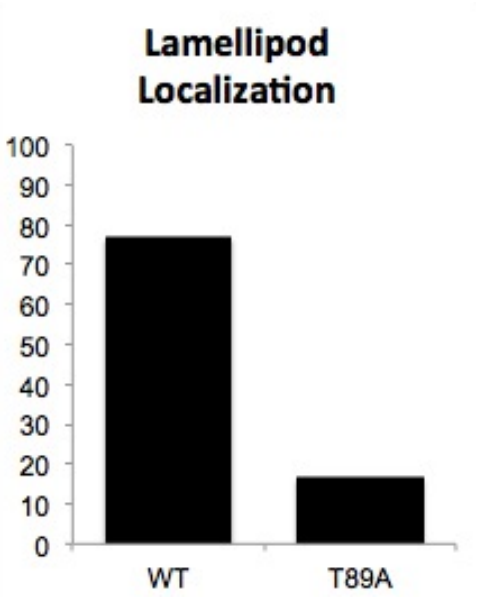

(b)

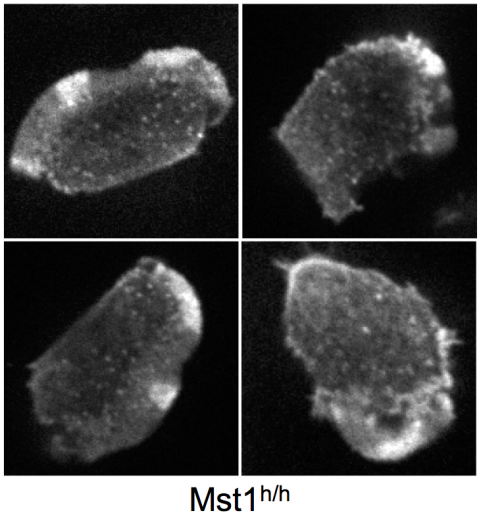

(c)

Figure 3.6. Phosphorylation of LPL Thr89 is required for proper lamellipodial localization and organization **(A,B)**Wt LPL or phosphorylation-resistant T89A LPL were transfected into purified $LPL^{-/-}$ CD4 T-cells. Cells were allowed to migrated on ICAM-1 coated surface before fixation and stained with rhodamine-phalloidin. A spinning-disk confocal microscope was used to capture photos of both transfection. Blinded scoring of LPL lamellipodia localization and lamellipodia formation were scored (B). **(C)**Purified $Mst1^{h/h}$ CD4 T-cellswere fixed and stained with rhodamine-phalloidin to visualize F-actin structures.

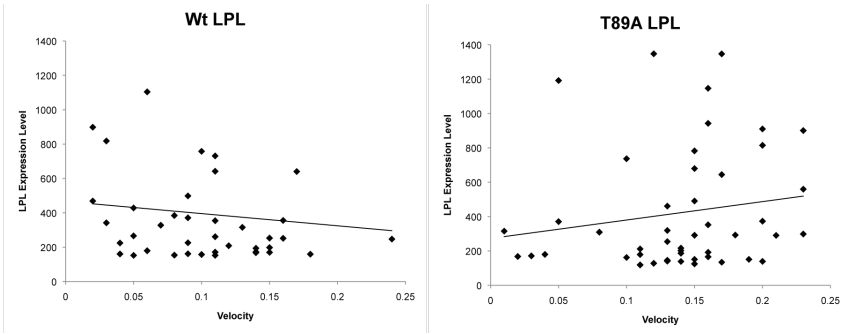

(a)

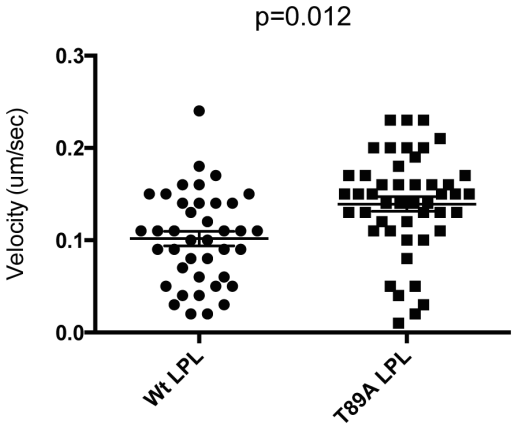

(b)

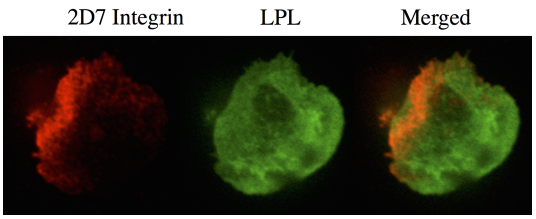

(c)

Figure 3.7. Phosphorylation of LPL Thr89 is required for proper lamellipodial localization and organization **(A,B)**Wt LPL or phosphorylation-resistant T89A LPL were transfected into purified $LPL^{-/-}$ CD4 T-cells. Cells were allowed to migrated on ICAM-1 coated surface before fixation and stained with rhodamine-phalloidin. A spinning-disk confocal microscope was used to capture photos of both transfection. Blinded scoring of LPL lamellipodia localization and lamellipodia formation were scored (B).

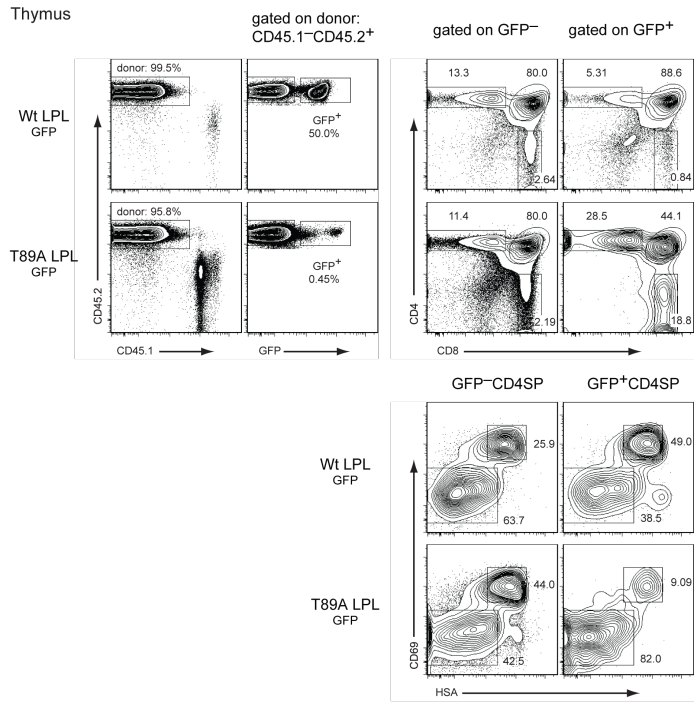

(a)

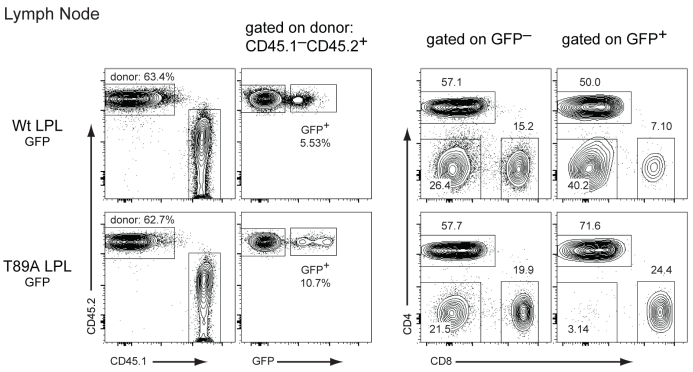

(b)

Figure 3.8. Phosphorylation of LPL Thr89 is required for proper lamellipodial localization and organization **(A,B)**Wt LPL or phosphorylation-resistant T89A LPL were transfected into purified LPL$^{-/-}$ CD4 T-cells. Cells were allowed to migrated on ICAM-1 coated surface before fixation and stained with rhodamine-phalloidin. A spinning-disk confocal microscope was used to capture photos of both transfection. Blinded scoring of LPL lamellipodia localization and lamellipodia formation were scored (B).

4. Summary and Future Directions

4.1 Summary of Thesis

Using ENU-induced mutagenesis, a mouse harboring a single nucleotide mutation in the Mst1 gene was identified by flow-cytometry in a screen for peripheral immune system defects. This mouse model led us to investigate the function of Mst1 kinase in T-cell migration. Prior publications had indicated a polarization defect and an integrin-clustering defect in T-cells lacking Mst1 in response to chemokine-induced inside-out signaling. However, no study has yet uncovered the molecular mechanisms underlying the Mst1-dependent polarization and integrin-clustering pathway. We set out to search for the missing molecular links between Mst1 and the physical process of polarization and integrin clustering. Since Mst1 is a kinase, we decided to pursue its potential phosphorylation substrates and ask whether any substrate can connect the pathway. With this in mind, we used different methods to search for potential substrates, including comparative phospho-proteomics done on wildtype and Mst1-deficient T cells, and evaluation of gene knockout mouse models that phenocopied the Mst1 mutant model. With these approaches, we identified a group of potential candidates in cytoskeleton regulation. Among

them, we chose the actin-bundling protein L-plastin as a potential target, because L-plastin knockout mice exhibited a similar thymic egress block as Mst1 mutant mice, and the protein is known to control integrin activation and leukocyte polarization. Using *in vitro* kinase assay with purified recombinant Mst1 and L-plastin proteins, we identified threonine 89 on L-plastin to be an Mst1 phosphorylation site. We also validated physiological interactions between the two proteins intracellularly with luciferase complementation assays. We then confirmed the physiological relevance of Mst1-L-plastin regulation pathway by generating bone marrow chimeras with L-plastin knockout hematopoietic stem cells reconstituted with either wt or phosphorylation-resistant T89A L-plastin, and found that only the wt chimeras had normal thymic egress. Having determined *in vivo* that the phosphorylation site is biologically indispensable, we next found that at the single cell level that phosphorylation was important for proper lamellipodia localization and formation. We also found that wt but not T89A LPL enhanced T-cell adhesion to integrin ligands, suggesting a function in activating integrins. These results suggested two important cell-biological functions for Mst1 regulation of L-plastin: bundling actin in order to properly organize lamellipodia, and directly or indirectly activating integrin.

While we were studying the functions of L-plastin, a lingering question always remained with us: what is the molecular link between Mst1 and cell polarization? Having observed the different morphologies of wt and Mst1 mutant cells, we determined that the mutant cells had a "flappy" morphology and

usually occupied more space on coverslips than wt cells, signaling a decreased intracellular tension, reminiscent of myosin-inhibited cells. We then carefully compared the mutant cells with wt cells treated with blebbistatin, a highly specific inhibitor for myosin contractility. They both had increased percentages of non-polarized cells. When they did polarize, they were more likely to be multipolar, characterized by more than one lamellipodia. Additionally, we found that neither Mst1-deficient cells nor blebbistatin-treated cells were able to distribute low affinity LFA-1 integrin properly. Based on these extensive similarities, we then asked whether Mst1 could directly regulate and activate myosin. Because MRLC2 represents the best studied mechanism of myosin regulation, we examined whether its protein sequence had site(s) for Mst1 phosphorylation with an online library and its scoring tool. Subsequently with purified recombinant Mst1 kinase and MRLC2, we carried out *in vitro* kinase assay and identified MRLC T10 and T11 as sites for Mst1 phosphorylation. Similar to LPL, we also validated intracellular interaction with luciferase complementation assays.

4.2 Future Directions

At the current stage, there are still many unanswered questions. For instance, where in the cell does Mst1 phosphorylate L-plastin, at the front edge or at the mid-body? The front edge is where L-plastin bundles F-actin and facilitate the formation of lamellipodium, whereas the mid-body is where high

affinity integrins are situated. Therefore, Mst1 can phosphorylate L-plastin at d location and let it carry out its function. On the other hand, these two functions can be a continual process such that extension and contraction of lamellipodium at the front leads to the activation of integrin and strengthening of firm adhesion at the mid-body. Another question is whether L-plastin directly or indirectly activates integrin. There was one study [137] showing that L-plastin could directly bind to integrin β chain. We have, however, not been able to repeat the experiment in the absence of cross-linking reagents. Other experiments, such as luciferase complementation assay or Forster resonance energy transfer assay (FRET) between integrin chains and L-plastin can be carried out in live cells to answer the question more accurately. We also would like to use electron-microscopy to observe the ultra-structures of the abnormal actin in lamellipodium with T89A L-plastin and gauge the physical processes behind the phosphorylation site. As for the regulation of myosin activity by Mst1, we would like to see what physiological role phosphorylation of T10/11 by Mst1 plays in promoting myosin activity, and whether phosphomimic T10/11E can rescue polarization defect in Mst1 mutant cells. Overall, both L-plastin and MRLC2 fit the described phenotypes of Mst1 mutant cells very well, and we would like to figure out the underlying biophysics of their actions.

5. References

[1] Ulrich H. von Andrian and Charles R. Mackay. T-cell function and migration — two sides of the same coin. *New England Journal of Medicine*, 343(14):1020–1034, 2000. PMID: 11018170.

[2] C H Kim and H E Broxmeyer. Chemokines: signal lamps for trafficking of t and b cells for development and effector function. *J Leukoc Biol*, 65(1):6–15, Jan 1999.

[3] J G Cyster. Chemokines and cell migration in secondary lymphoid organs. *Science*, 286(5447):2098–2102, Dec 1999.

[4] A Zlotnik and O Yoshie. Chemokines: a new classification system and their role in immunity. *Immunity*, 12(2):121–127, Feb 2000.

[5] Ulrich H von Andrian and Thorsten R Mempel. Homing and cellular traffic in lymph nodes. *Nat Rev Immunol*, 3(11):867–878, Nov 2003.

[6] H B Jr Stamper and J J Woodruff. An in vitro model of lymphocyte homing. i. characterization of the interaction between thoracic duct lymphocytes and specialized high-endothelial venules of lymph nodes. *J Immunol*, 119(2):772–780, Aug 1977.

[7] J P Girard and T A Springer. High endothelial venules (hevs): specialized endothelium for lymphocyte migration. *Immunol Today*, 16(9):449–457, Sep 1995.

[8] Bing-Hao Luo, Christopher V Carman, and Timothy A Springer. Structural basis of integrin regulation and signaling. *Annu Rev Immunol*, 25:619–647, 2007.

[9] Tatsuo Kinashi. Intracellular signalling controlling integrin activation in lymphocytes. *Nat Rev Immunol*, 5(7):546–559, Jul 2005.

[10] Nancy Hogg, Irene Patzak, and Frances Willenbrock. The insider's guide to leukocyte integrin signalling and function. *Nat Rev Immunol*, 11(6):416–426, Jun 2011.

[11] Myrto Raftopoulou and Alan Hall. Cell migration: Rho gtpases lead the way. *Dev Biol*, 265(1):23–32, Jan 2004.

[12] Anne J Ridley, Martin A Schwartz, Keith Burridge, Richard A Firtel, Mark H Ginsberg, Gary Borisy, J Thomas Parsons, and Alan Rick Horwitz. Cell migration: integrating signals from front to back. *Science*, 302(5651):1704–1709, Dec 2003.

[13] C D Nobes and A Hall. Rho, rac, and cdc42 gtpases regulate the assembly of multimolecular focal complexes associated with actin stress fibers, lamellipodia, and filopodia. *Cell*, 81(1):53–62, Apr 1995.

[14] Marcus Thelen and Jens V Stein. How chemokines invite leukocytes to dance. *Nat Immunol*, 9(9):953–9, Sep 2008.

[15] Thomas D Pollard and John A Cooper. Actin, a central player in cell shape and movement. *Science*, 326(5957):1208–1212, Nov 2009.

[16] Matthew F Krummel and Ian Macara. Maintenance and modulation of t cell polarity. *Nat Immunol*, 7(11):1143–1149, Nov 2006.

[17] Sharon Celeste Morley. The actin-bundling protein l-plastin supports t-cell motility and activation. *Immunol Rev*, 256(1):48–62, Nov 2013.

[18] Nils C Gauthier, Thomas A Masters, and Michael P Sheetz. Mechanical feedback between membrane tension and dynamics. *Trends Cell Biol*, 22(10):527–535, Oct 2012.

[19] J Thomas Parsons, Alan Rick Horwitz, and Martin A Schwartz. Cell adhesion: integrating cytoskeletal dynamics and cellular tension. *Nat Rev Mol Cell Biol*, 11(9):633–43, Sep 2010.

[20] Jorg Renkawitz and Michael Sixt. Mechanisms of force generation and force transmission during interstitial leukocyte migration. *EMBO Rep*, 11(10):744–750, Oct 2010.

[21] Dylan T Burnette, Suliana Manley, Prabuddha Sengupta, Rachid Sougrat, Michael W Davidson, Bechara Kachar, and Jennifer Lippincott-

Schwartz. A role for actin arcs in the leading-edge advance of migrating cells. *Nat Cell Biol*, 13(4):371–381, Apr 2011.

[22] Colin K Choi, Miguel Vicente-Manzanares, Jessica Zareno, Leanna A Whitmore, Alex Mogilner, and Alan Rick Horwitz. Actin and alpha-actinin orchestrate the assembly and maturation of nascent adhesions in a myosin ii motor-independent manner. *Nat Cell Biol*, 10(9):1039–1050, Sep 2008.

[23] Dylan T Burnette, Lin Shao, Carolyn Ott, Ana M Pasapera, Robert S Fischer, Michelle A Baird, Christelle Der Loughian, Helene Delanoe-Ayari, Matthew J Paszek, Michael W Davidson, Eric Betzig, and Jennifer Lippincott-Schwartz. A contractile and counterbalancing adhesion system controls the 3d shape of crawling cells. *J Cell Biol*, 205(1):83–96, Apr 2014.

[24] A Ponti, M Machacek, S L Gupton, C M Waterman-Storer, and G Danuser. Two distinct actin networks drive the protrusion of migrating cells. *Science*, 305(5691):1782–1786, Sep 2004.

[25] Ke Hu, Lin Ji, Kathryn T Applegate, Gaudenz Danuser, and Clare M Waterman-Storer. Differential transmission of actin motion within focal adhesions. *Science*, 315(5808):111–115, Jan 2007.

[26] Gregory Giannone, Benjamin J Dubin-Thaler, Olivier Rossier, Yunfei Cai, Oleg Chaga, Guoying Jiang, William Beaver, Hans-Gunther

Dobereiner, Yoav Freund, Gary Borisy, and Michael P Sheetz. Lamellipodial actin mechanically links myosin activity with adhesion-site formation. *Cell*, 128(3):561–575, Feb 2007.

[27] Alexander D Bershadsky, Nathalie Q Balaban, and Benjamin Geiger. Adhesion-dependent cell mechanosensitivity. *Annu Rev Cell Dev Biol*, 19:677–695, 2003.

[28] C E Turner. Paxillin and focal adhesion signalling. *Nat Cell Biol*, 2(12):E231–6, Dec 2000.

[29] Jean-Cheng Kuo, Xuemei Han, Cheng-Te Hsiao, John R 3rd Yates, and Clare M Waterman. Analysis of the myosin-ii-responsive focal adhesion proteome reveals a role for beta-pix in negative regulation of focal adhesion maturation. *Nat Cell Biol*, 13(4):383–393, Apr 2011.

[30] Pakorn Kanchanawong, Gleb Shtengel, Ana M Pasapera, Ericka B Ramko, Michael W Davidson, Harald F Hess, and Clare M Waterman. Nanoscale architecture of integrin-based cell adhesions. *Nature*, 468(7323):580–584, Nov 2010.

[31] D A Lauffenburger and A F Horwitz. Cell migration: a physically integrated molecular process. *Cell*, 84(3):359–69, Feb 1996.

[32] Nicole A Morin, Patrick W Oakes, Young-Min Hyun, Dooyoung Lee, Y Eugene Chin, Michael R King, Timothy A Springer, Motomu Shi-

maoka, Jay X Tang, Jonathan S Reichner, and Minsoo Kim. Nonmuscle myosin heavy chain iia mediates integrin lfa-1 de-adhesion during t lymphocyte migration. *J Exp Med*, 205(1):195–205, Jan 2008.

[33] Paula Stanley, Andrew Smith, Alison McDowall, Alastair Nicol, Daniel Zicha, and Nancy Hogg. Intermediate-affinity lfa-1 binds alpha-actinin-1 to control migration at the leading edge of the t cell. *EMBO J*, 27(1):62–75, Jan 2008.

[34] Andrew Smith, Yolanda R Carrasco, Paula Stanley, Nelly Kieffer, Facundo D Batista, and Nancy Hogg. A talin-dependent lfa-1 focal zone is formed by rapidly migrating t lymphocytes. *J Cell Biol*, 170(1):141–51, Jul 2005.

[35] Bodo Borm, Robert P Requardt, Volker Herzog, and Gregor Kirfel. Membrane ruffles in cell migration: indicators of inefficient lamellipodia adhesion and compartments of actin filament reorganization. *Exp Cell Res*, 302(1):83–95, Jan 2005.

[36] P Friedl, S Borgmann, and E B Bröcker. Amoeboid leukocyte crawling through extracellular matrix: lessons from the dictyostelium paradigm of cell movement. *J Leukoc Biol*, 70(4):491–509, Oct 2001.

[37] Alex Mogilner, Jun Allard, and Roy Wollman. Cell polarity: quantitative modeling as a tool in cell biology. *Science*, 336(6078):175–9, Apr 2012.

[38] Chin-Jen Ku, Yanqin Wang, Orion D Weiner, Steven J Altschuler, and Lani F Wu. Network crosstalk dynamically changes during neutrophil polarization. *Cell*, 149(5):1073–83, May 2012.

[39] Angela H Chau, Jessica M Walter, Jaline Gerardin, Chao Tang, and Wendell A Lim. Designing synthetic regulatory networks capable of self-organizing cell polarization. *Cell*, 151(2):320–32, Oct 2012.

[40] Jordan Jacobelli, Rachel S Friedman, Mary Anne Conti, Ana-Maria Lennon-Dumenil, Matthieu Piel, Caitlin M Sorensen, Robert S Adelstein, and Matthew F Krummel. Confinement-optimized three-dimensional t cell amoeboid motility is modulated via myosin iia-regulated adhesions. *Nat Immunol*, 11(10):953–61, Oct 2010.

[41] Ronen Alon and Michael L Dustin. Force as a facilitator of integrin conformational changes during leukocyte arrest on blood vessels and antigen-presenting cells. *Immunity*, 26(1):17–27, Jan 2007.

[42] Ziv Shulman, Vera Shinder, Eugenia Klein, Valentin Grabovsky, Orna Yeger, Erez Geron, Alessio Montresor, Matteo Bolomini-Vittori, Sara W Feigelson, Tomas Kirchhausen, Carlo Laudanna, Guy Shakhar, and Ronen Alon. Lymphocyte crawling and transendothelial migration require chemokine triggering of high-affinity lfa-1 integrin. *Immunity*, 30(3):384–96, Mar 2009.

[43] Koko Katagiri, Masakazu Hattori, Nagahiro Minato, and Tatsuo Kinashi. Rap1 functions as a key regulator of t-cell and antigen-presenting cell interactions and modulates t-cell responses. *Mol Cell Biol*, 22(4):1001–15, Feb 2002.

[44] K A Reedquist, E Ross, E A Koop, R M Wolthuis, F J Zwartkruis, Y van Kooyk, M Salmon, C D Buckley, and J L Bos. The small gtpase, rap1, mediates cd31-induced integrin adhesion. *J Cell Biol*, 148(6):1151–8, Mar 2000.

[45] K Suga, K Katagiri, T Kinashi, M Harazaki, T Iizuka, M Hattori, and N Minato. Cd98 induces lfa-1-mediated cell adhesion in lymphoid cells via activation of rap1. *FEBS Lett*, 489(2-3):249–53, Feb 2001.

[46] Mika Shimonaka, Koko Katagiri, Toshinori Nakayama, Naoya Fujita, Takashi Tsuruo, Osamu Yoshie, and Tatsuo Kinashi. Rap1 translates chemokine signals to integrin activation, cell polarization, and motility across vascular endothelium under flow. *J Cell Biol*, 161(2):417–27, Apr 2003.

[47] J L Bos, J de Rooij, and K A Reedquist. Rap1 signalling: adhering to new models. *Nat Rev Mol Cell Biol*, 2(5):369–77, May 2001.

[48] Monika Raab, Xin Smith, Yves Matthess, Klaus Strebhardt, and Christopher E Rudd. Skap1 protein ph domain determines rapl mem-

brane localization and rap1 protein complex formation for t cell receptor (tcr) activation of lfa-1. *J Biol Chem*, 286(34):29663–70, Aug 2011.

[49] Koko Katagiri, Noriko Ohnishi, Kenji Kabashima, Tomonori Iyoda, Naoki Takeda, Yoichi Shinkai, Kayo Inaba, and Tatsuo Kinashi. Crucial functions of the rap1 effector molecule rapl in lymphocyte and dendritic cell trafficking. *Nat Immunol*, 5(10):1045–51, Oct 2004.

[50] Yukihiko Ebisuno, Koko Katagiri, Tomoya Katakai, Yoshihiro Ueda, Tomomi Nemoto, Hiroyuki Inada, Junichi Nabekura, Takaharu Okada, Reiji Kannagi, Toshiyuki Tanaka, Masayuki Miyasaka, Nancy Hogg, and Tatsuo Kinashi. Rap1 controls lymphocyte adhesion cascade and interstitial migration within lymph nodes in rapl-dependent and -independent manners. *Blood*, 115(4):804–814, Jan 2010.

[51] Koko Katagiri, Akito Maeda, Mika Shimonaka, and Tatsuo Kinashi. Rapl, a rap1-binding molecule that mediates rap1-induced adhesion through spatial regulation of lfa-1. *Nat Immunol*, 4(8):741–8, Aug 2003.

[52] Koko Katagiri, Masashi Imamura, and Tatsuo Kinashi. Spatiotemporal regulation of the kinase mst1 by binding protein rapl is critical for lymphocyte polarity and adhesion. *Nat Immunol*, 7(9):919–28, Sep 2006.

[53] Jieqing Zhu, Christopher V Carman, Minsoo Kim, Motomu Shimaoka, Timothy A Springer, and Bing-Hao Luo. Requirement of alpha and beta

subunit transmembrane helix separation for integrin outside-in signaling. *Blood*, 110(7):2475–2483, Oct 2007.

[54] Benjamin Geiger, Joachim P Spatz, and Alexander D Bershadsky. Environmental sensing through focal adhesions. *Nat Rev Mol Cell Biol*, 10(1):21–33, Jan 2009.

[55] Donna J Webb, Karen Donais, Leanna A Whitmore, Sheila M Thomas, Christopher E Turner, J Thomas Parsons, and Alan F Horwitz. Fak-src signalling through paxillin, erk and mlck regulates adhesion disassembly. *Nat Cell Biol*, 6(2):154–61, Feb 2004.

[56] Satyajit K Mitra, Daniel A Hanson, and David D Schlaepfer. Focal adhesion kinase: in command and control of cell motility. *Nat Rev Mol Cell Biol*, 6(1):56–68, Jan 2005.

[57] Clare L Abram and Clifford A Lowell. The ins and outs of leukocyte integrin signaling. *Annu Rev Immunol*, 27:339–62, 2009.

[58] Yolanda R Carrasco, Sebastian J Fleire, Thomas Cameron, Michael L Dustin, and Facundo D Batista. Lfa-1/icam-1 interaction lowers the threshold of b cell activation by facilitating b cell adhesion and synapse formation. *Immunity*, 20(5):589–99, May 2004.

[59] Minsoo Kim, Christopher V Carman, Wei Yang, Azucena Salas, and Timothy A Springer. The primacy of affinity over clustering in regulation

of adhesiveness of the integrin alphalbeta2. *J Cell Biol*, 167(6):1241–1253, Dec 2004.

[60] Renhao Li, Neal Mitra, Holly Gratkowski, Gaston Vilaire, Rustem Litvinov, Chandrasekaran Nagasami, John W Weisel, James D Lear, William F DeGrado, and Joel S Bennett. Activation of integrin alphaiibbeta3 by modulation of transmembrane helix associations. *Science*, 300(5620):795–798, May 2003.

[61] Paola Chiarugi and Elisa Giannoni. Anoikis: a necessary death program for anchorage-dependent cells. *Biochem Pharmacol*, 76(11):1352–64, Dec 2008.

[62] Xingfeng Bao, E Ashley Moseman, Hideo Saito, Bronislawa Petryniak, Aude Thiriot, Shingo Hatakeyama, Yuki Ito, Hiroto Kawashima, Yu Yamaguchi, John B Lowe, Ulrich H von Andrian, and Minoru Fukuda. Endothelial heparan sulfate controls chemokine presentation in recruitment of lymphocytes and dendritic cells to lymph nodes. *Immunity*, 33(5):817–829, Nov 2010.

[63] M D Gunn, K Tangemann, C Tam, J G Cyster, S D Rosen, and L T Williams. A chemokine expressed in lymphoid high endothelial venules promotes the adhesion and chemotaxis of naive t lymphocytes. *Proc Natl Acad Sci U S A*, 95(1):258–263, Jan 1998.

[64] Ziv Shulman, Shmuel J Cohen, Ben Roediger, Vyacheslav Kalchenko, Rohit Jain, Valentin Grabovsky, Eugenia Klein, Vera Shinder, Liat Stoler-Barak, Sara W Feigelson, Tsipi Meshel, Susanna M Nurmi, Itamar Goldstein, Olivier Hartley, Carl G Gahmberg, Amos Etzioni, Wolfgang Weninger, Adit Ben-Baruch, and Ronen Alon. Transendothelial migration of lymphocytes mediated by intraendothelial vesicle stores rather than by extracellular chemokine depots. *Nat Immunol*, 13(1):67–76, Jan 2012.

[65] J W Homeister, A D Thall, B Petryniak, P Maly, C E Rogers, P L Smith, R J Kelly, K M Gersten, S W Askari, G Cheng, G Smithson, R M Marks, A K Misra, O Hindsgaul, U H von Andrian, and J B Lowe. The alpha(1,3)fucosyltransferases fuct-iv and fuct-vii exert collaborative control over selectin-dependent leukocyte recruitment and lymphocyte homing. *Immunity*, 15(1):115–126, Jul 2001.

[66] Tim Lammermann, Bernhard L Bader, Susan J Monkley, Tim Worbs, Roland Wedlich-Soldner, Karin Hirsch, Markus Keller, Reinhold Forster, David R Critchley, Reinhard Fassler, and Michael Sixt. Rapid leukocyte migration by integrin-independent flowing and squeezing. *Nature*, 453(7191):51–55, May 2008.

[67] Silvia F Soriano, Miroslav Hons, Kathrin Schumann, Varsha Kumar, Timo J Dennier, Ruth Lyck, Michael Sixt, and Jens V Stein. In vivo

analysis of uropod function during physiological t cell trafficking. *J Immunol*, 187(5):2356–2364, Sep 2011.

[68] Duojia Pan. The hippo signaling pathway in development and cancer. *Dev Cell*, 19(4):491–505, Oct 2010.

[69] Sirio Dupont, Leonardo Morsut, Mariaceleste Aragona, Elena Enzo, Stefano Giulitti, Michelangelo Cordenonsi, Francesca Zanconato, Jimmy Le Digabel, Mattia Forcato, Silvio Bicciato, Nicola Elvassore, and Stefano Piccolo. Role of yap/taz in mechanotransduction. *Nature*, 474(7350):179–83, Jun 2011.

[70] Mariaceleste Aragona, Tito Panciera, Andrea Manfrin, Stefano Giulitti, Federica Michielin, Nicola Elvassore, Sirio Dupont, and Stefano Piccolo. A mechanical checkpoint controls multicellular growth through yap/taz regulation by actin-processing factors. *Cell*, 154(5):1047–59, Aug 2013.

[71] Jixin Dong, Georg Feldmann, Jianbin Huang, Shian Wu, Nailing Zhang, Sarah A Comerford, Mariana F Gayyed, Robert A Anders, Anirban Maitra, and Duojia Pan. Elucidation of a universal size-control mechanism in drosophila and mammals. *Cell*, 130(6):1120–1133, Sep 2007.

[72] Marius Sudol and Kieran F Harvey. Modularity in the hippo signaling pathway. *Trends Biochem Sci*, 35(11):627–33, Nov 2010.

[73] Boon Chuan Low, Catherine Qiurong Pan, G V Shivashankar, Alexander Bershadsky, Marius Sudol, and Michael Sheetz. Yap/taz as mechanosensors and mechanotransducers in regulating organ size and tumor growth. *FEBS Lett*, Apr 2014.

[74] Bin Zhao, Li Li, Karen Tumaneng, Cun-Yu Wang, and Kun-Liang Guan. A coordinated phosphorylation by lats and ck1 regulates yap stability through scf(beta-trcp). *Genes Dev*, 24(1):72–85, Jan 2010.

[75] Fa-Xing Yu, Bin Zhao, Nattapon Panupinthu, Jenna L Jewell, Ian Lian, Lloyd H Wang, Jiagang Zhao, Haixin Yuan, Karen Tumaneng, Hairi Li, Xiang-Dong Fu, Gordon B Mills, and Kun-Liang Guan. Regulation of the hippo-yap pathway by g-protein-coupled receptor signaling. *Cell*, 150(4):780–91, Aug 2012.

[76] Koko Katagiri, Tomoya Katakai, Yukihiko Ebisuno, Yoshihiro Ueda, Takaharu Okada, and Tatsuo Kinashi. Mst1 controls lymphocyte trafficking and interstitial motility within lymph nodes. *EMBO J*, 28(9):1319–31, May 2009.

[77] Dahu Chen, Yutong Sun, Yongkun Wei, Peijing Zhang, Abdol Hossein Rezaeian, Julie Teruya-Feldstein, Sumeet Gupta, Han Liang, Hui-Kuan Lin, Mien-Chie Hung, and Li Ma. Lifr is a breast cancer metastasis suppressor upstream of the hippo-yap pathway and a prognostic marker. *Nat Med*, 18(10):1511–7, Oct 2012.

[78] Nam-Gyun Kim, Eunjin Koh, Xiao Chen, and Barry M Gumbiner. E-cadherin mediates contact inhibition of proliferation through hippo signaling-pathway components. *Proc Natl Acad Sci U S A*, 108(29):11930–11935, Jul 2011.

[79] Bin Zhao, Li Li, Lloyd Wang, Cun-Yu Wang, Jindan Yu, and Kun-Liang Guan. Cell detachment activates the hippo pathway via cytoskeleton reorganization to induce anoikis. *Genes Dev*, 26(1):54–68, Jan 2012.

[80] Fan Mou, Maria Praskova, Fan Xia, Denille Van Buren, Hanno Hock, Joseph Avruch, and Dawang Zhou. The mst1 and mst2 kinases control activation of rho family gtpases and thymic egress of mature thymocytes. *J Exp Med*, 209(4):741–59, Apr 2012.

[81] Yongli Dong, Xingrong Du, Jian Ye, Min Han, Tian Xu, Yuan Zhuang, and Wufan Tao. A cell-intrinsic role for mst1 in regulating thymocyte egress. *J Immunol*, 183(6):3865–72, Sep 2009.

[82] Nadine T Nehme, Jana Pachlopnik Schmid, Franck Debeurme, Isabelle André-Schmutz, Annick Lim, Patrick Nitschke, Frédéric Rieux-Laucat, Patrick Lutz, Capucine Picard, Nizar Mahlaoui, Alain Fischer, and Geneviève de Saint Basile. Mst1 mutations in autosomal recessive primary immunodeficiency characterized by defective naive t-cell survival. *Blood*, 119(15):3458–68, Apr 2012.

[83] Amandine Crequer, Capucine Picard, Etienne Patin, Aurelia D'Amico, Avinash Abhyankar, Martine Munzer, Marianne Debré, Shen-Ying Zhang, Geneviève de Saint-Basile, Alain Fischer, Laurent Abel, Gérard Orth, Jean-Laurent Casanova, and Emmanuelle Jouanguy. Inherited mst1 deficiency underlies susceptibility to ev-hpv infections. *PLoS One*, 7(8):e44010, 2012.

[84] Hengameh Abdollahpour, Giridharan Appaswamy, Daniel Kotlarz, Jana Diestelhorst, Rita Beier, Alejandro A Schäffer, E Michael Gertz, Axel Schambach, Hans H Kreipe, Dietmar Pfeifer, Karin R Engelhardt, Nima Rezaei, Bodo Grimbacher, Sabine Lohrmann, Roya Sherkat, and Christoph Klein. The phenotype of human stk4 deficiency. *Blood*, 119(15):3450–7, Apr 2012.

[85] David Masopust and Jason M Schenkel. The integration of t cell migration, differentiation and function. *Nat Rev Immunol*, 13(5):309–20, May 2013.

[86] Michael G Overstreet, Alison Gaylo, Bastian R Angermann, Angela Hughson, Young-Min Hyun, Kris Lambert, Mridu Acharya, Alison C Billroth-Maclurg, Alexander F Rosenberg, David J Topham, Hideo Yagita, Minsoo Kim, Adam Lacy-Hulbert, Martin Meier-Schellersheim, and Deborah J Fowell. Inflammation-induced interstitial migration of ef-

fector cd4 t cells is dependent on integrin v. *Nat Immunol*, 14(9):949–58, Sep 2013.

[87] Yoshihiro Ueda, Koko Katagiri, Takashi Tomiyama, Kaneki Yasuda, Katsuyoshi Habiro, Tomoya Katakai, Susumu Ikehara, Mitsuru Matsumoto, and Tatsuo Kinashi. Mst1 regulates integrin-dependent thymocyte trafficking and antigen recognition in the thymus. *Nat Commun*, 3:1098, 2012.

[88] Stefanie Kliche, Tim Worbs, Xiaoqian Wang, Janine Degen, Irene Patzak, Bernhard Meineke, Mauro Togni, Markus Moser, Annegret Reinhold, Friedemann Kiefer, Christian Freund, Reinhold Förster, and Burkhart Schraven. Ccr7-mediated lfa-1 functions in t cells are regulated by 2 independent adap/skap55 modules. *Blood*, 119(3):777–85, Jan 2012.

[89] Andrew Smith, Paula Stanley, Kristian Jones, Lena Svensson, Alison McDowall, and Nancy Hogg. The role of the integrin lfa-1 in t-lymphocyte migration. *Immunol Rev*, 218:135–46, Aug 2007.

[90] Miguel Vicente-Manzanares, Xuefei Ma, Robert S Adelstein, and Alan Rick Horwitz. Non-muscle myosin ii takes centre stage in cell adhesion and migration. *Nat Rev Mol Cell Biol*, 10(11):778–790, Nov 2009.

[91] Jordan Jacobelli, F Chris Bennett, Priya Pandurangi, Aaron J Tooley, and Matthew F Krummel. Myosin-iia and icam-1 regulate the inter-

change between two distinct modes of t cell migration. *J Immunol*, 182(4):2041–50, Feb 2009.

[92] Sharona Even-Ram, Andrew D Doyle, Mary Anne Conti, Kazue Matsumoto, Robert S Adelstein, and Kenneth M Yamada. Myosin iia regulates cell motility and actomyosin-microtubule crosstalk. *Nat Cell Biol*, 9(3):299–309, Mar 2007.

[93] Miguel Vicente-Manzanares, Karen Newell-Litwa, Alexia I Bachir, Leanna A Whitmore, and Alan Rick Horwitz. Myosin iia/iib restrict adhesive and protrusive signaling to generate front-back polarity in migrating cells. *J Cell Biol*, 193(2):381–96, Apr 2011.

[94] Jordan Jacobelli, Miriam Estin Matthews, Stephanie Chen, and Matthew F Krummel. Activated t cell trans-endothelial migration relies on myosin-iia contractility for squeezing the cell nucleus through endothelial cell barriers. *PLoS One*, 8(9):e75151, 2013.

[95] Gerard F Hoyne and Christopher C Goodnow. The use of genomewide enu mutagenesis screens to unravel complex mammalian traits: identifying genes that regulate organ-specific and systemic autoimmunity. *Immunol Rev*, 210:27–39, Apr 2006.

[96] Yina Hsing Huang, Rina Barouch-Bentov, Ann Herman, John Walker, and Karsten Sauer. Integrating traditional and postgenomic approaches

to investigate lymphocyte development and function. *Adv Exp Med Biol*, 584:245–76, 2006.

[97] Tim Wiltshire, Mathew T Pletcher, Serge Batalov, S Whitney Barnes, Lisa M Tarantino, Michael P Cooke, Hua Wu, Kevin Smylie, Andrey Santrosyan, Neal G Copeland, Nancy A Jenkins, Francis Kalush, Richard J Mural, Richard J Glynne, Steve A Kay, Mark D Adams, and Colin F Fletcher. Genome-wide single-nucleotide polymorphism analysis defines haplotype patterns in mouse. *Proc Natl Acad Sci U S A*, 100(6):3380–5, Mar 2003.

[98] K F Manly, R H Cudmore, Jr, and J M Meer. Map manager qtx, cross-platform software for genetic mapping. *Mamm Genome*, 12(12):930–2, Dec 2001.

[99] Mathew T Pletcher, Philip McClurg, Serge Batalov, Andrew I Su, S Whitney Barnes, Erica Lagler, Ron Korstanje, Xiaosong Wang, Deborah Nusskern, Molly A Bogue, Richard J Mural, Beverly Paigen, and Tim Wiltshire. Use of a dense single nucleotide polymorphism map for in silico mapping in the mouse. *PLoS Biol*, 2(12):e393, Dec 2004.

[100] F Sánchez-Madrid and M A del Pozo. Leukocyte polarization in cell migration and immune interactions. *EMBO J*, 18(3):501–11, Feb 1999.

[101] Andrew Smith, Madelon Bracke, Birgit Leitinger, Joanna C Porter, and Nancy Hogg. Lfa-1-induced t cell migration on icam-1 involves regulation

of mlck-mediated attachment and rock-dependent detachment. *J Cell Sci*, 116(Pt 15):3123–33, Aug 2003.

[102] Yang Wang, Dan Li, Roza Nurieva, Justin Yang, Mehmet Sen, Roberto Carreño, Sijie Lu, Bradley W McIntyre, Jeffrey J Molldrem, Glen B Legge, and Qing Ma. Lfa-1 affinity regulation is necessary for the activation and proliferation of naive t cells. *J Biol Chem*, 284(19):12645–53, May 2009.

[103] Aaron F Straight, Amy Cheung, John Limouze, Irene Chen, Nick J Westwood, James R Sellers, and Timothy J Mitchison. Dissecting temporal and spatial control of cytokinesis with a myosin ii inhibitor. *Science*, 299(5613):1743–7, Mar 2003.

[104] Martin Lee Miller, Lars Juhl Jensen, Francesca Diella, Claus Jørgensen, Michele Tinti, Lei Li, Marilyn Hsiung, Sirlester A Parker, Jennifer Bordeaux, Thomas Sicheritz-Ponten, Marina Olhovsky, Adrian Pasculescu, Jes Alexander, Stefan Knapp, Nikolaj Blom, Peer Bork, Shawn Li, Gianni Cesareni, Tony Pawson, Benjamin E Turk, Michael B Yaffe, Søren Brunak, and Rune Linding. Linear motif atlas for phosphorylation-dependent signaling. *Sci Signal*, 1(35):ra2, 2008.

[105] Eiji Kinoshita, Emiko Kinoshita-Kikuta, and Tohru Koike. Separation and detection of large phosphoproteins using phos-tag sds-page. *Nat Protoc*, 4(10):1513–21, 2009.

[106] Kathryn E Luker and David Piwnica-Worms. Optimizing luciferase protein fragment complementation for bioluminescent imaging of protein-protein interactions in live cells and animals. *Methods Enzymol*, 385:349–60, 2004.

[107] David A Calderwood, Iain D Campbell, and David R Critchley. Talins and kindlins: partners in integrin-mediated adhesion. *Nat Rev Mol Cell Biol*, 14(8):503–17, Aug 2013.

[108] Yanling Chen, Bingwen Lu, Qingkai Yang, Colleen Fearns, John R Yates, 3rd, and Jiing-Dwan Lee. Combined integrin phosphoproteomic analyses and small interfering rna–based functional screening identify key regulators for cancer cell adhesion and migration. *Cancer Res*, 69(8):3713–20, Apr 2009.

[109] Eilon Woolf, Irina Grigorova, Adi Sagiv, Valentin Grabovsky, Sara W Feigelson, Ziv Shulman, Tanja Hartmann, Michael Sixt, Jason G Cyster, and Ronen Alon. Lymph node chemokines promote sustained t lymphocyte motility without triggering stable integrin adhesiveness in the absence of shear forces. *Nat Immunol*, 8(10):1076–85, Oct 2007.

[110] Tim Lämmermann and Michael Sixt. Mechanical modes of 'amoeboid' cell migration. *Curr Opin Cell Biol*, 21(5):636–44, Oct 2009.

[111] Michael L Dustin. T-cell activation through immunological synapses and kinapses. *Immunol Rev*, 221:77–89, Feb 2008.

[112] Xin Liu, Tarun M Kapoor, James K Chen, and Morgan Huse. Diacylglycerol promotes centrosome polarization in t cells via reciprocal localization of dynein and myosin ii. *Proc Natl Acad Sci U S A*, 110(29):11976–81, Jul 2013.

[113] Jason Yi, Xufeng S Wu, Travis Crites, and John A Hammer, 3rd. Actin retrograde flow and actomyosin ii arc contraction drive receptor cluster dynamics at the immunological synapse in jurkat t cells. *Mol Biol Cell*, 23(5):834–52, Mar 2012.

[114] Morgan Huse, Audrey Le Floc'h, and Xin Liu. From lipid second messengers to molecular motors: microtubule-organizing center reorientation in t cells. *Immunol Rev*, 256(1):95–106, Nov 2013.

[115] Jordan R Beach, Lucila S Licate, James F Crish, and Thomas T Egelhoff. Analysis of the role of ser1/ser2/thr9 phosphorylation on myosin ii assembly and function in live cells. *BMC Cell Biol*, 12:52, 2011.

[116] Jason G Cyster and Susan R Schwab. Sphingosine-1-phosphate and lymphocyte egress from lymphoid organs. *Annu Rev Immunol*, 30:69–94, 2012.

[117] Y Namba, M Ito, Y Zu, K Shigesada, and K Maruyama. Human t cell l-plastin bundles actin filaments in a calcium-dependent manner. *J Biochem*, 112(4):503–507, Oct 1992.

[118] Sharon Celeste Morley, Chen Wang, Wan-Lin Lo, Chan-Wang J Lio, Bernd H Zinselmeyer, Mark J Miller, Eric J Brown, and Paul M Allen. The actin-bundling protein l-plastin dissociates ccr7 proximal signaling from ccr7-induced motility. *J Immunol*, 184(7):3628–38, Apr 2010.

[119] Michael Freeley, Francis O'Dowd, Toby Paul, Dmitry Kashanin, Anthony Davies, Dermot Kelleher, and Aideen Long. L-plastin regulates polarization and migration in chemokine-stimulated human t lymphocytes. *J Immunol*, 188(12):6357–70, Jun 2012.

[120] Chen Wang, Sharon Celeste Morley, David Donermeyer, Ivan Peng, Wyne P Lee, Jason Devoss, Dimitry M Danilenko, Zhonghua Lin, Juan Zhang, Jie Zhou, Paul M Allen, and Eric J Brown. Actin-bundling protein l-plastin regulates t cell activation. *J Immunol*, 185(12):7487–97, Dec 2010.

[121] S L Jones and E J Brown. Fcgammarii-mediated adhesion and phagocytosis induce l-plastin phosphorylation in human neutrophils. *J Biol Chem*, 271(24):14623–30, Jun 1996.

[122] S L Jones, J Wang, C W Turck, and E J Brown. A role for the actin-bundling protein l-plastin in the regulation of leukocyte integrin function. *Proc Natl Acad Sci U S A*, 95(16):9331–6, Aug 1998.

[123] J Wang and E J Brown. Immune complex-induced integrin activation and l-plastin phosphorylation require protein kinase a. *J Biol Chem*, 274(34):24349–56, Aug 1999.

[124] Bassam Janji, Adeline Giganti, Veerle De Corte, Marie Catillon, Erik Bruyneel, Delphine Lentz, Julie Plastino, Jan Gettemans, and Evelyne Friederich. Phosphorylation on ser5 increases the f-actin-binding activity of l-plastin and promotes its targeting to sites of actin assembly in cells. *J Cell Sci*, 119(Pt 9):1947–60, May 2006.

[125] Pere Roca-Cusachs, Armando del Rio, Eileen Puklin-Faucher, Nils C Gauthier, Nicolas Biais, and Michael P Sheetz. Integrin-dependent force transmission to the extracellular matrix by -actinin triggers adhesion maturation. *Proc Natl Acad Sci U S A*, 110(15):E1361–70, Apr 2013.

[126] Ronen Zaidel-Bar, Christoph Ballestrem, Zvi Kam, and Benjamin Geiger. Early molecular events in the assembly of matrix adhesions at the leading edge of migrating cells. *J Cell Sci*, 116(Pt 22):4605–13, Nov 2003.

[127] Johannes Schindelin, Ignacio Arganda-Carreras, Erwin Frise, Verena Kaynig, Mark Longair, Tobias Pietzsch, Stephan Preibisch, Curtis Rueden, Stephan Saalfeld, Benjamin Schmid, Jean-Yves Tinevez, Daniel James White, Volker Hartenstein, Kevin Eliceiri, Pavel Toman-

cak, and Albert Cardona. Fiji: an open-source platform for biological-image analysis. *Nat Methods*, 9(7):676–82, Jul 2012.

[128] Marc R Block, Cedric Badowski, Angelique Millon-Fremillon, Daniel Bouvard, Anne-Pascale Bouin, Eva Faurobert, Delphine Gerber-Scokaert, Emmanuelle Planus, and Corinne Albiges-Rizo. Podosome-type adhesions and focal adhesions, so alike yet so different. *Eur J Cell Biol*, 87(8-9):491–506, Sep 2008.

[129] Dorit Hanein and Alan Rick Horwitz. The structure of cell-matrix adhesions: the new frontier. *Curr Opin Cell Biol*, 24(1):134–40, Feb 2012.

[130] E Zamir and B Geiger. Molecular complexity and dynamics of cell-matrix adhesions. *J Cell Sci*, 114(Pt 20):3583–90, Oct 2001.

[131] Ewa Stepniak, Glenn L Radice, and Valeri Vasioukhin. Adhesive and signaling functions of cadherins and catenins in vertebrate development. *Cold Spring Harb Perspect Biol*, 1(5):a002949, Nov 2009.

[132] Tony J C Harris and Ulrich Tepass. Adherens junctions: from molecules to morphogenesis. *Nat Rev Mol Cell Biol*, 11(7):502–14, Jul 2010.

[133] Sara W Feigelson, Ronit Pasvolsky, Saso Cemerski, Ziv Shulman, Valentin Grabovsky, Tal Ilani, Adi Sagiv, Fabrice Lemaitre, Carlo Laudanna, Andrey S Shaw, and Ronen Alon. Occupancy of lymphocyte lfa-1 by surface-immobilized icam-1 is critical for tcr- but not for chemokine-

triggered lfa-1 conversion to an open headpiece high-affinity state. *J Immunol*, 185(12):7394–404, Dec 2010.

[134] Christopher V Carman, Peter T Sage, Tracey E Sciuto, Miguel A de la Fuente, Raif S Geha, Hans D Ochs, Harold F Dvorak, Ann M Dvorak, and Timothy A Springer. Transcellular diapedesis is initiated by invasive podosomes. *Immunity*, 26(6):784–97, Jun 2007.

[135] Ziad Al Tanoury, Elisabeth Schaffner-Reckinger, Aliaksandr Halavatyi, Céline Hoffmann, Michèle Moes, Ermin Hadzic, Marie Catillon, Mikalai Yatskou, and Evelyne Friederich. Quantitative kinetic study of the actin-bundling protein l-plastin and of its impact on actin turn-over. *PLoS One*, 5(2):e9210, 2010.

[136] Guido H Wabnitz, Philipp Lohneis, Henning Kirchgessner, Beate Jahraus, Susan Gottwald, Mathias Konstandin, Martin Klemke, and Yvonne Samstag. Sustained lfa-1 cluster formation in the immune synapse requires the combined activities of l-plastin and calmodulin. *Eur J Immunol*, 40(9):2437–49, Sep 2010.

[137] E Le Goff, A Vallentin, P-O Harmand, G Aldrian-Herrada, B Rebière, C Roy, Y Benyamin, and M-C Lebart. Characterization of l-plastin interaction with beta integrin and its regulation by micro-calpain. *Cytoskeleton (Hoboken)*, 67(5):286–96, May 2010.